

Beyond Universal Approximation Theorems: Algorithmic Uniform Approximation by Neural Networks Trained with Noisy Data

Anastasis Kratsios*

Tin Sum Cheng†

Daniel Roy‡

Abstract

At its core, machine learning seeks to train models that reliably generalize beyond noisy observations; however, the theoretical vacuum in which state-of-the-art universal approximation theorems (UATs) operate isolates them from this goal, as they assume noiseless data and allow network parameters to be chosen freely, independent of algorithmic realism. This paper bridges that gap by introducing an architecture-specific randomized training algorithm that constructs a uniform approximator from N noisy training samples on the d -dimensional cube $[0, 1]^d$. Our trained neural networks attain the minimax-optimal quantity of *trainable* (non-random) parameters, subject to logarithmic factors which vanish under the idealized noiseless sampling assumed in classical UATs.

Additionally, our trained models replicate key behaviours of real-world neural networks, absent in standard UAT constructions, by: (1) exhibiting sub-linear parametric complexity when fine-tuning on structurally related and favourable out-of-distribution tasks, (2) exactly interpolating the training data, and (3) maintaining reasonable Lipschitz regularity (after the initial clustering attention layer). These properties bring state-of-the-art UATs closer to practical machine learning, shifting the central open question from algorithmic implementability with noisy samples to whether stochastic gradient descent can achieve comparable guarantees.

Keywords: Algorithmic Universal Approximation, Universal Approximation, Noisy Training Data, Generalization.
MSC (2020) Classification: 68T07, 68Q32, 68T05, 41A65

1 Introduction

The goal of machine learning is to algorithmically identify models that generalize beyond their training data, even in the presence of measurement noise, and a central aim of AI theory is to ensure the reliability of these trained models. One pillar of AI theory are the *universal approximation theorems* (UATs), which guarantee that the neural network backbones of these AI can uniformly approximate any continuous function locally on Euclidean space. Since their earliest concurrent formulations [54, 28, 45], UATs have remained in an isolated theoretical vacuum, assuming *noiseless* data and affording users the unrealistic ability to freely select network parameters independently of *algorithmic realism* and of statistical pragmatism. Consequently, the networks constructed even by modern UATs remain disconnected from the goals of AI practice and learning theory. Additionally, state-of-the-art UATs do not produce networks sharing many well-documented properties of real-world trained neural networks, such as their capacity to generalize on related out-of-distribution tasks with minimal fine-tuning cost.

Although a unified theory, fully explaining modern deep learning architectures trained with contemporary stochastic gradient descent still remains well-beyond the reach of the AI theory community, there are several meaningful intermediate advances to be made. This paper resolves a number of those intermediate steps and effectively merging *approximation theory* with the goals of *learning theory*. This conceptual and technical shift is best understood in the context of the contemporary approximation theory paradigm for deep learning

1.1 Deficits With the State-of-the-art in Neural Network Approximation Theory

We juxtapose our results and our approach by reviewing the state-of-the-art in modern neural network approximation theory, as summarized in Table 1. The existing methods for constructing neural network approximators can be broadly classified into five categories: 1) classical existence theorems, which guarantee the asymptotic representational power of certain architectures without providing explicit constructions; 2) constructive approximation results, which specify how to build networks by borrowing tools from constructive approximation theory [74]; 3) random linearization

*Department of Mathematics, McMaster University, Canada; kratsioa@mcmaster.ca

†Department of Mathematics and Computer Science, University of Basel, Switzerland; tinsum.cheng@unibas.ch

‡Department of Statistical Sciences, University of Toronto, Canada; Vector Institute, Canada; daniel.roy@utoronto.ca

techniques, which regress against random untrained hidden features; 4) methods inspired by compressed sensing, which use MLPs to build and regress against sparse polynomial bases, and 5) methods which build Riesz bases of neural network bases dictionary and linearly regress thereon. Table 1 contrasts these method, against real-world deep learning architectures trained with stochastic gradient descent-type algorithms (SGD), and against our theory.

Approach	Optimal Rates ¹	Approx.	Worst-Case (Uniform)	Implementable Algorithm	Label-Noise	Training Interpolation	Scalable Fine-Tuning (OOD)	References
Qualitative Existence	NA		✓	×	×	×	×	[54, 28, 60]
Constructive Apprx.	✓		✓	×	×	✓/×	×	[113, 88, 16, 50, 101, 117, 52, 96]
Kernalization (RFN & NTK)	×		×	✓	×	??	×	[48, 47, 80, 23, 21, 22]
Compressed Sensing Emulation	✓		×	≈	×	×	×	[18, 17, 43, 102]
Lin. Reg w. MLP Basis	✓		✓	✓	×	×	×	[29, 99, 98]
Ours: Algorithmic Approximation	✓		✓	✓	✓	✓	✓	This Paper
Real NNs (SGD)	??		??	✓	??	??	??	NA

Table 1: Comparative summary of NNs approximator constructions.

Classical existence theorems, i.e., the classical UAT [54, 28, 60], guarantee the existence of a sufficiently large neural network that can approximate any given target function to arbitrary accuracy. However, they offer no guidance on how to identify such a model from data, nor do they specify its size or neuronal structure.

Guarantees based on constructive approximation, especially [113, 88, 16, 50, 101, 96], improve upon this by providing estimates for the number of neurons and their arrangement (in terms of depth, width, and number of active neurons) required to approximate a function of a given regularity to a specified precision. Although these results do not explicitly rely on finitely many samples, later refinements, cf. [117, 52], do. While these approaches achieve minimax-optimal approximation rates, as dictated by matching lower-bounds in constructive approximation theory [74] and Vapnik-Chervonenkis theory [113, 101], they rely on precisely placed samples without measurement noise. All these guarantees break down when either of these two assumptions is violated, which is almost always the practical use cases. Furthermore, although these results do provide a (semi-)explicit architectural construction, their architectural constructions are far too elaborate to implement by any realistic training algorithm. Similar issues arise with the optimal memorization theorems which are finite counterparts to these results; cf. [108, 61, 64, 34, 78].

Random feature networks (RFNs) [94] address some of these limitations by randomizing all but the final layer of a neural network, which is then trained via linear, or ridge, regression. This stylized linearization enables the tractable analysis of their L^2 -approximation power [47, 85] and statistical behaviour [48, 80], by reducing them to kernel methods for which a comprehensive statistical theory is by now well-developed [23, 21, 22]. Neural tangent kernels (NTKs) [58, 46] further narrow the gap between RFNs and practical neural networks by incorporating gradient dynamics through the analysis of infinitely wide network surrogates. While these approaches provide indispensable insight into trained deep neural networks, the linearization they rely on necessarily eliminates the core non-linearity, granting neural networks their expressive power. This gap between linearized and non-linear networks is rigorously articulated by the mismatch between the best known lower bounds for non-linear approximation (cf. linear widths [91]) and the best upper bounds (cf. various notions of non-linear widths [31, 25, 90]). Similar performance gaps have also been documented in the statistical literature between RFNs and two-layer neural networks with one step of gradient training on their hidden features; cf. [37, 84]. Additionally, RFNs and NTKs typically guarantee only (squared-)average performance on noisy data, without worst-case uniform guarantees; a critical limitation for deep learning in sciences facing rare extreme events, e.g., fluid dynamics [30], climate [104], and actuarial [38] science.

Recently, progress has been made toward concretely trainable neural networks that achieve optimal approximation rates, albeit on idealized training data. Two parallel directions have emerged, both of which construct large dictionaries of basic functions (e.g., neural networks) and then perform linear regression over that dictionary. The first direction emulates classical compressed sensing results by constructing optimal polynomial bases using expressive ReLU² networks [18, 17, 43, 102]. These models enjoy near-optimal approximation rates, admit training via ridge regression, and can accommodate randomly sampled inputs. The second direction [29, 99, 98] follows a similar strategy, but builds large dictionaries consisting of Riesz bases for standard function spaces that can be realized by very simple ReLU MLPs; sparse linear regression over this dictionary then yields an effective approximator. While the first approach accommodates finitely many noiseless but randomly located input samples, neither direction currently handles random measurement noise in the setting where uniform approximation of the target function is desired.

More broadly, a key gap in these theoretical foundations is that the three fundamental facets of deep learning models—architectural expressiveness, statistical biases, and optimization, are routinely studied in mutual-isolation rather than concurrently. This fragmentation of the deep learning pipeline leads to loose theoretical results by decoupling these three factors, whose synchronicity is popularly understood as being responsible for the success of modern AIs. Perhaps more concerning, is that the isolated treatment of approximation from *learning theory*

naturally inspires degenerate approximation results [115, 118, 59] constructing neural network with exorbitantly fast approximation rates at the cost of an infinite VC/pseudo-dimension (cf. [101, Theorem 2.4]), i.e. these models are not PAC learnable² [15]. Simultaneously, these, although interesting, result necessarily forge any training stability needed for stable function reconstruction of from corrupted training data; contracting the *optimization* lens implicitly present in classical numerical analysis wisdom [32, 31, 25, 90].

1.2 Primary Contribution: Algorithmic Approximation Under Measurement Noise

Our main contribution is an *architecture-specific*, randomized *training algorithm* (Algorithms 1, 2, and 3) that outputs networks which can provably **uniformly approximate** any continuous ground truth function given finitely many noisy (randomly placed) training samples (Theorem 5.1). Consequently, our primary contribution bridges uniform approximation theorems and learning guarantees for a specific deep neural network architecture (cf. Figure 1) trained with a fully explicit algorithm. Importantly, we do not rely on oracle inequalities that decouple learning and approximation, e.g. [100, 79, 68, 97]; instead, we analyze a concrete neural network training pipeline in which the optimization, approximation, and statistical components are tightly integrated. In this way, our main result addresses each of the major deficits of the aforementioned approximation theories (cf. Table 1).

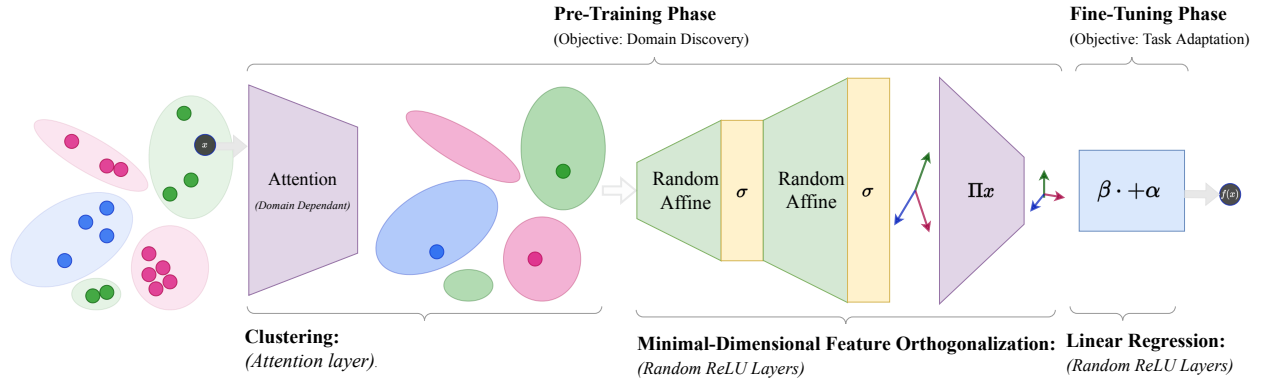


Figure 1: The structure of the three-phase transformers trained with Algorithms 1, 2, and 3:

Phase 0 – Denoising (Algorithm 1): In the preliminary denoising phase, an approximately noise-free dataset is formed by locally averaging the original noisy samples, allowing downstream training to use near-true function values. This step can be omitted if no measurement noise is present, as in universal approximation theorems; e.g. [101].

Phase 1 – Clustering (Algorithm 2): In the *clustering phase*, our trained transformer maps inputs in $[0, 1]^d$ to representatives of a set of discovered clusters (illustrated by points in distinct colours). Each cluster is represented by a single point that summarizes (possibly disjoint) regions of the domain that are both close in input space and have similar target values in the range (Proposition 4.2).

Phase 2 – Minimal-Dimension Feature Orthogonalization (Algorithm 3): Next, carefully generated randomized ReLU MLP and unactivated affine layers, are used to orthogonalized each cluster’s representative point in the lowest possible dimension. This is because the trained deep feature matrix is well-conditions with high probability (Proposition 4.3). This orthogonalization guarantees that the downstream linear regression in the network’s final layer admits a solution, while the minimal dimension ensures that this solution is unique.

Phase 3 – Linear Regression (Trained): Lastly, the final layer is trained via standard linear regression on the learned deep features. Owing to their structure, this enables the neural network to interpolate each representative cluster with its associated cluster value in the range, while simultaneously ensuring that the regressor possesses high Lipschitz regularity (Theorem 5.1).

Our training algorithm is *tailored* to the three-phase *transformer* model summarized in Figure 1. As a byproduct, our main result sheds insight on how transformers operate and, specifically, what operations attention mechanisms effectively compute³. We exhibit a neural network architecture and propose a concrete, *architecture-specific*, randomized *end-to-end training algorithm* that learns network parameters implementing a uniform approximator of the ground truth function; even when trained on noisy data. Unlike RFN and NTK approaches, our training procedure

²Strictly speaking, binary classifiers constructed using a $I_{(0, \infty)}$ final layer are not PAC-learnable.

³The attention mechanism at the first layer of our architecture can be replaced by a deep ReLU MLP computing the maximum function (cf. [89, Lemma 5.11]). However, the resulting architecture would lose algorithmic transparency, which is one of our main desiderata.

(Algorithms 1, 2, 3) trains the first layer, enabling adaptation to the domain’s structure—something the rigid, *non-adaptive* hidden features of RFNs and NTKs cannot achieve their hidden layers being fixed after (random) initialization. Our use of a minimal representation dimension, after phase 2, grants us interpolation even with ridgeless regression; which need not be possible with high-dimensional feature representations; cf. [22].

We underscore that this paper’s contribution is not intended as a scalable black-box training algorithm that resolves these challenges for general neural network architectures. Rather, our objective is exhibit a pair of a deep learning architecture and a plausible training algorithm resolving all of the *open problems* listed in Table 1.

The Denoising Algorithm A central contribution of this paper, and key step in bridging approximation theory and practical machine learning is our Algorithm 1. This pre-processing method provably reduces measurement noise in training data with high probability given sufficiently large sample sizes and is of independent interest, as it can be incorporated into other deep learning pipelines and theoretical analyses. This step can be omitted in the absence of measurement noise, in which case we recover the setting of most compressed sensing–based UATs (cf. [18, 17, 43, 102]). If, in addition, the user is granted the ability to select the locations at which noiseless samples are observed, then we recover the setting of state-of-the-art UATs in constructive approximation (cf. [113, 88, 101, 52]).

1.3 Secondary Contributions: Sub-Linear OOD Fine-Tuning via Symmetries

An indicator that our proposed theory may be a step in the right direction toward explaining deep learning, beyond what is offered by the classical approximation theoretic-lens, is its success in account for other empirically observed phenomena. Beyond guaranteed *benign interpolation*⁴ of the training data (Theorem 5.1) our analysis reveals novel *combinatorial symmetries* (Definition 3.3), a stylized property of image data (cf. Section 3.1), that permit the use of low-dimensional linear regression output layers (see Figure 1). When the target function possesses sufficient symmetry, the dimension of the output layer can scale sub-linearly as $\mathcal{O}(\varepsilon^{-r})$ for some dimension-free $0 < r < 1$, in sharp contrast to the $\Theta(\varepsilon^{-d})$ rate required for optimal approximation by generic ReLU networks lacking such structure [101, 52]. Leveraging this structure, our transformer can be efficiently *fine-tuned* allowing it adapt to new, but structurally, out-of-distributional regression tasks by only retraining only the *final layer* via standard regression, upon refining the new task’s training dataset by running Algorithm 1. This yields a *dimension-free* number of parameters to be re-trained during OOD fine-tuning which $\mathcal{O}(\varepsilon^{-r})$, which significantly improves classical approaches would require retraining $\Theta(\varepsilon^{-d})$ parameters.

Leveraging these results, we show that a sample complexity of $\mathcal{O}(1/N^r) \ll \mathcal{O}(1/N)$ is achievable for any OOD regression task that shares the same combinatorial symmetries as the pre-training task (Corollary 5.1). This yields strictly faster rates than those obtainable via classical assumptions such as log-concavity of the data distribution [33] or standard margin conditions [106, 9]. Moreover, our bounds are dimension-free and do not require the data-generating distribution to satisfy a log-Sobolev inequality [40, 20] (cf. [71]).

Finally, we show that combinatorial symmetries are not merely a theoretical construct but are both empirically prevalent in standard image datasets (see Section 3.1) and mathematically inevitable due to Ramsey-theoretic principles (Proposition 3.1). Our combinatorial symmetries offer a complementary form of regularity that neural networks can exploit—distinct from the strong smoothness assumptions commonly used in scientific computing inspired deep learning [4, 19, 27], and more amenable to practical verification than compositional assumptions on the target function [92, 97, 24, 93].

Further Implication: Algorithmic Construction of Neural Network Memorizers We note that when provided with noiseless training data our algorithm implies a randomized polynomial-time procedure for constructing a three-layer MLP capable of memorizing any finite regression dataset. Unlike the result of [34], our approach is not restricted to binary classification. Moreover, unlike [78, 110], this sub-result is algorithmic rather than merely existential, and it does not require any stylized separation conditions on the input; only that the input data points are distinct. Unlike each of these results, our construction is an additionally a uniform approximator.

1.4 Further Related Works: Beyond Approximation Theory

Most other lenses on the foundations of AI also operate by considering one step of the standard deep learning pipeline in isolation from the others. For instance PAC-learning results [5, 26] typically disregard the training algorithm

⁴We purposefully do not refer to this *benign overfitting* since, unlike in benign overfitting (cf. [44, 62, 105]), we are provably not *overfitting*. Our main result (Theorem 5.1) guarantees uniform approximation/reconstruction of the ground truth function—and *not* of the ground truth function plus noise.

entirely, focusing instead on worst-case generalization guarantees over excessively large model classes [70, 13, 12, 36], or rely on surrogate randomized models [7, 35, 39, 111] whose relevance in practice may be limited without further de-randomization. Each of these frameworks also typically omits at least one of the core ingredients of practical supervised learning: 1) dependence on the specific training data; 2) finite, noisy datasets; and 3) evaluation via uniform recovery of the true target function, not merely up to additive noise. In contrast, our main result takes a first step toward a unified theoretical foundation by integrating approximation, statistical, and optimization considerations into a single deep learning model, providing concrete and provable guarantees.

Organization of Paper

All preliminary definitions and notational conventions are introduced in Section 2. Section 3.3 then motivates and formalizes our notion of combinatorial symmetries, and demonstrates their prevalence in standard image datasets. Our three-phase training algorithm is presented in Section 4, with each step accompanied by an explanation of its key properties. The main theoretical results appear in Section 5, followed by a discussion in Section 6. All proofs and additional technical details are provided in the appendices.

2 Preliminaries and Definitions

We now formalize the key background concepts underlying our main results and algorithms. This includes a precise specification of the transformer model shown in Figure 1, as well as a brief discussion of the distinct notions of ground truth reconstruction (i.e., risk minimization versus uniform approximation). We also collect notation.

2.1 Our Transformer Model

We formalize the transformer model illustrated in Figure 1. Our attention mechanism is of standard type with two simple tweaks: 1) we consider ℓ^∞ -based alignment of any incoming query to the contextual keys instead of angle-based (cosine similarity) alignment⁵ and 2) we take the temperature to infinity. With these modifications our *max-temperature* attention mechanism, is defined for any $d_k, d_v \in \mathbb{N}_+$, and $d \times d_k$ *keys* matrix K , and any $d_v \times d_k$ *values* matrix V by $\text{Attn}(\cdot|K, V) : \mathbb{R}^d \rightarrow \mathbb{R}^C$ and mapping any input *query* $x \in \mathbb{R}^d$ to the following *context score* in \mathbb{R}^d by ranking its ℓ^∞ distance-based alignment score with the keys K_1, \dots, K_{d_k} populating the columns of K as follows

$$\underbrace{\text{Attn}(x|K, V)}_{\text{Context Vector}} \stackrel{\text{def.}}{=} \underbrace{\overbrace{V}^{\text{Values}}}_{\text{Context Vector}} \text{Softmax}_\infty \left(\underbrace{- \bigoplus_{i=1}^{d_k} \left\| \overbrace{x}^{\text{Queries}} - \overbrace{K_i}^{\text{Keys}} \right\|_\infty}_{\substack{\text{Alignment Scores:} \\ \text{Ranks Alignment to training data-point(s)}}} \right) \quad (1)$$

where the *max-temperature softmax* function is the pointwise limit of the softmax function as temperature tends to infinity, defined for any $z \in \mathbb{R}^{d_k}$

$$\text{Softmax}_\infty((z_i)_{i=1}^{d_k}) \stackrel{\text{def.}}{=} \left(\frac{I_{z_i = \max_{u \in [d_k]} z_u} z_u}{\# \arg\max_{u \in [d_k]} z_u} \right)_{i=1}^{d_k}. \quad (2)$$

Consider the two-layer randomized neural network $\hat{f} : \mathbb{R}^d \rightarrow \mathbb{R}^D$ defined for each $x \in \mathbb{R}^d$ by

$$\begin{aligned} \hat{f}(x) &= \beta \mathcal{E}(x) \\ \mathcal{E}(x) &\stackrel{\text{def.}}{=} \frac{1}{\sqrt{Fp^{(2)}}} \Pi \text{ReLU} \left(B^{(2)} \frac{1}{\sqrt{Fp^{(1)}}} \text{ReLU} (B^{(1)} z + b^{(1)}) + b^{(2)} \right) \\ z &\stackrel{\text{def.}}{=} \text{Attn}(x|K, V) \end{aligned} \quad (3)$$

for hidden width F and feature dimension $W \in \mathbb{N}_+$, matrices $\beta : \mathbb{R}^{D \times F}$, $\Pi^{W \times F}$, $B^{(1)} \in \mathbb{R}^{d \times F}$, and $B^{(2)}$, biases $b^{(1)}, b^{(2)} \in \mathbb{R}^F$, and hyper-parameters $p^{(1)}, p^{(2)} > 0$ (to be specified later determined by the biases). Note that, Π defines an unbiased and unactivated linear layer. Our main result is intimately tied to the well-conditioning of the (random) *deep feature matrix* defined by

$$\mathbb{X}_{\mathcal{E}, \mathcal{D}} \stackrel{\text{def.}}{=} \mathbf{1}_\kappa \oplus (\mathcal{E}(u_1), \dots, \mathcal{E}(u_K)) \quad (4)$$

⁵Note the same analysis would likely work for cosine similarities if data is normalized to the sphere. In which case, cosine similarities are the distance function associated to the usual (Procrustes) Riemannian metric thereon.

where $\mathcal{D} = \{(X_n, Y_n)\}_{n=1}^K$ is a (possibly noisy) training set and $\mathcal{E} : \mathbb{R}^d \rightarrow \mathbb{R}^D$ outputs the peri-ultimate layer/logits of the transformer of the form (3).

2.2 What Are Good Signal-Reconstruction Metrics?

A learner is typically considered to have learned if its in-sample performance on the training task reliably predicts its out-of-sample performance on new data drawn from the same task. We now present two formalizations of this notion. The first, framed in terms of the size of the *generalization gap* and arises in classical statistical learning theory. The second, is the uniform approximation error, which is rooted in approximation theory.

Given a τ -training set $\mathcal{D} \stackrel{\text{def.}}{=} \{(X_n, Y_n)\}_{n=1}^N$, the gap between training and testing is formalized by the discrepancy between the *true risk* $\mathcal{R}(\hat{f})$ and *empirical risk* $\hat{\mathcal{R}}_{\mathcal{D}}(\hat{f})$ for a given learner $\hat{f} : \mathbb{R}^d \rightarrow \mathbb{R}^D$; as defined by

$$\mathcal{R}(\hat{f}) \stackrel{\text{def.}}{=} \mathbb{E}_{X \sim \mathbb{P}_X, \varepsilon \sim \mathbb{P}_\varepsilon} [\|\hat{f}(X) - (f(X) + \varepsilon)\|] \text{ and } \hat{\mathcal{R}}_{\mathcal{D}}(\hat{f}) \stackrel{\text{def.}}{=} \frac{1}{N} \sum_{n=1}^N \|\hat{f}(X_n) - Y_n\| \quad (5)$$

where, we use the root-mean-squared-error as a quantifier of the error size. A central goal of classical learning theory is to guarantee that the worst-case *generalization gap*

$$|\mathcal{R}(\hat{f}) - \hat{\mathcal{R}}_{\mathcal{D}}(\hat{f})| \quad (6)$$

over all relevant learners \hat{f} asymptotically vanishes as the sample size N grows arbitrarily large. Importantly, this vanishing does not imply that any particular learner \hat{f} accurately reproduces the target function f ; rather, it ensures that its in-sample and out-of-sample performance are comparable. Consequently, if one can establish the existence of some learner \hat{f} that performs well on a given training set—e.g., via a universal approximation theorem (UAT)—then one may confidently infer that, on average, it can accurately reproduce the target function f blurred by noise ε .

Modern learning-theoretic techniques, e.g. [11, 86], guarantee that for many classes of neural networks with fixed parametric complexity (i.e., fixed depth, width, and maximal weight norm), the generalization gap (6) converges at a dimension-free rate matching the $\mathcal{O}(\frac{1}{\sqrt{N}})$ optimal rate of the central limit theorem; see, e.g., Sudakov’s minorant theorem and [69, Theorem 3.18]. However, these results do not guarantee that the same rate holds when network complexity grows. Such growth is necessary to ensure the existence of a neural network that can keep empirical risk small as the sample size increases; cf. the optimal memorization/interpolation results of [108, Theorem 1.1] and [64, Lemma 20], as well as the VC-dimensional lower bounds of [12].

When scaling the network size, one should instead expect the convergence of the generalization gap in (6) to behave similarly to the fat-shattering dimension of the class of learners [6, Theorem 3.6], which is comparable to its VC-dimension, and which must grow at a rate depending exponentially on the dimension d by [101, Theorem 2.4].

Our main result (Theorem 5.1) constructs a new training set by removing noise from the original data using Algorithm 1. Then, Algorithms 2 and 3 train a neural network that achieves zero empirical risk on this new dataset and small true risk (computed on the de-noised target data). In fact, we show not only that the true risk converges, but also that the *uniform approximation error* of the ground-truth function f converges; this is defined by

$$\mathcal{A}(\hat{f}) \stackrel{\text{def.}}{=} \sup_{x \in [0,1]^d} \|\hat{f}(x) - f(x)\|. \quad (7)$$

The latter challenge, driving $\mathcal{A}(\hat{f})$ to zero, is fundamentally harder than merely minimizing the generalization gap $|\mathcal{R}(\hat{f}) - \hat{\mathcal{R}}_{\mathcal{D}}|$. Indeed, the uniform approximation error (7) vanishes only when the ground-truth function f is faithfully reconstructed despite the presence of measurement noise, whereas the generalization gap (6) vanishes as soon as a learner’s in-sample performance on noisy data mirrors its out-of-sample performance on other noisy data; without ever guaranteeing recovery of the underlying noiseless function f . In this paper we address the harder task of controlling (7) in the presence of noisy training data, rather than the comparatively easier task of controlling (6).

3 Combinatorial Symmetries For Simple Out-of-Distributional Learning

We motivate our new technique for achieving favourable fine-tuning by identifying and leveraging novel stylized multiscale properties of image data. Consider Figure 2, where an image is coarsened at multiple scales by merging—or averaging—neighbouring pixels into superpixels; see, for example, [95, 41, 3, 77]. This process is analogous to the role of average-pooling filters in convolutional neural networks [72]. As we can see, several pixel values (greyscale colours)

are very frequently repeated; thus any model would not need to memorize a new value for each pixel but would rather need to first group pixels according to which colour “cluster” they belong to (e.g. black, dark grey, light grey, white) and then learn to memorize which cluster in the domain maps to which grey scale colour in the range. The location of pixels with the same values is considered a new type of “symmetry” (formalized in Section 3.3). Thus, the task in Figure 2 is an *inverse problem* seeking to colour each of the superpixels in the given image. Thus, the training data are a subset of coloured superpixels and the test data is the remaining masked *pixels*; here every image is viewed as a function on $[0, 1]^2$. Such inverse problem are prevalent in modern deep learning; see, e.g., [57, 87, 112].

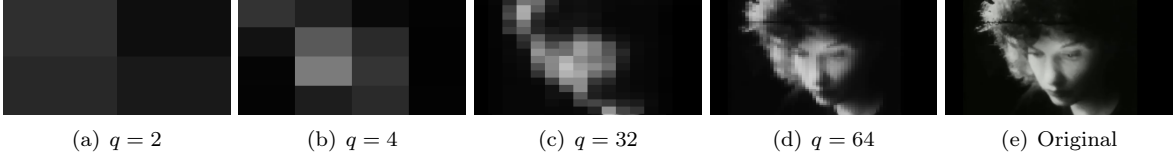


Figure 2: Coarsening of a typical greyscale image into q superpixel scales. Here, we have used 4, 16, 1024, 4096, pixels (q^2) from its original resolution (SubFigure 2(e)); a formal definition of this process is given in Section 3.1 using “averaging operators” on $L^2([0, 1]^d)$. *Image Credit: Maya Deren - Meshes of the Afternoon (1943)*.

3.1 Searching for Symmetries in Image Data

The core question on the viability of our symmetries hinges on their appearance in standard machine learning tasks such as *image classification* or *image-based regression* problems; which we now investigate. Let $q, \hbar \in \mathbb{N}_+$, let \mathcal{Q} be our set of sub-cubes of $[0, 1]^d$ with side-length $1/q$, and let $\frac{1}{\hbar}\mathbb{Z}^d \stackrel{\text{def.}}{=} \{z \in \mathbb{R}^d : \exists x \in \mathbb{Z}^d z = x/\hbar\}$ be the integer lattice rescaled by a factor reciprocal to \hbar . Define the discretization operator $\pi_{\hbar} : \mathbb{R}^D \rightarrow \frac{1}{\hbar}\mathbb{Z}^D$ rounding down any $z \in \mathbb{R}^D$ to the nearest re-scaled lattice point in $\frac{1}{\hbar}\mathbb{Z}^D$ by $\pi_{\hbar}(x) \stackrel{\text{def.}}{=} \{(z_i)_{i=1}^D : \max_{z_i \in \mathbb{Z}^d} z_i/\hbar \leq x_i\}$. For any cube $Q \in \mathcal{Q}$ denote the averaging operator $A_Q : L^1_{\text{loc}}([0, 1]) \rightarrow \mathbb{R}^D$ by

$$A_{Q,\hbar}(f) \stackrel{\text{def.}}{=} \pi_{\hbar} \left(\frac{1}{|Q|} \int_Q f(x) dx \right). \quad (8)$$

where $|Q| = q^{-d}$ denotes the (Lebesgue) volume of the cube and \int denotes the Bochner (componentwise-Lebesgue) integral. In the context of image processing, $A_{Q,\hbar}$ takes a group of pixels in an input image and creates a *superpixel* by coarsening, or averaging. The averaging operators $\{A_{Q,\hbar}\}_{Q \in \mathcal{Q}}$ allow us to approximate any function $f \in L^1([0, 1]^d)$ by a “coarseness” $f_{q,\hbar}$ version of the function f with they key property that: for each averaged cell-value (averaged by $A_{Q,\hbar}$) equals to the mid-point value of the coarsened function $f_{q,\hbar}$. In particular, this implies that the number of distinct and repeated values ascribed to the centre of any cube by the coarsened function equals to the number of cubes with a given average colour (according to $\{A_{Q,\hbar}\}_{Q \in \mathcal{Q}}$). These coarsened functions are defined as follows

$$f_{q,\hbar}(x) \stackrel{\text{def.}}{=} \sum_{Q \in \mathcal{Q}} A_{Q,\hbar}(f) \phi_{Q,\hbar}(x) \quad (9)$$

where $\phi_{Q,\hbar}(x) \stackrel{\text{def.}}{=} (1 - 2^{-\hbar} \|\bar{Q} - x\|_{\infty})_+$, \bar{Q} is the centre of the cube $Q \in \mathcal{Q}$ and $(u)_+ \stackrel{\text{def.}}{=} \max\{0, u\}$ for any $u \in \mathbb{R}$. As illustrated in Figure 2 in our paper’s introduction, these averaging operators (applied to each cell in a given image) operate by “coarsening” an input (e.g. an image) by averaging cells and rounding down their value to the re-scaled integer lattice $\frac{1}{\hbar}\mathbb{Z}^D$ (i.e. rounding down the grey-scale value), similar to *average pooling layers* in *convolutional neural networks*. Surprisingly, we see that the distinct number of possible greyscale colours, denoted by κ relative to the total number of cells q^2 , is close to zero, indicating that there is an overwhelmingly high number of repeated colours in image data. Though one should expect repeated values when we consider any continuous and “sufficiently bounded” function by the pigeonhole principle (if $q \gg \hbar$), our experiment shows that there are a surprisingly small number of distinct grey-scale colours; much fewer than one may expect from the pigeonhole principle alone.

The key point is that when we coarse-grain a function/image, then repetition becomes somewhat likely, as in the above figures, while one should not expect much represented in the continuum limit (original function) due to degenerate properties of the reals; i.e. $f_{q,\hbar}$ cannot fluctuate much making repeated values inescapable; e.g. by the pigeonhole principle if $\sqrt[d]{\hbar + 1} < q$ then $\kappa \stackrel{\text{def.}}{=} \#\{f_{q,\hbar}([0, 1]^d)\} \leq \hbar + 1$. More strikingly, is the *unavoidability* reality that arbitrarily long repetitions must happen, if q is large enough compared to \hbar , necessarily due to *Ramsey theoretic*

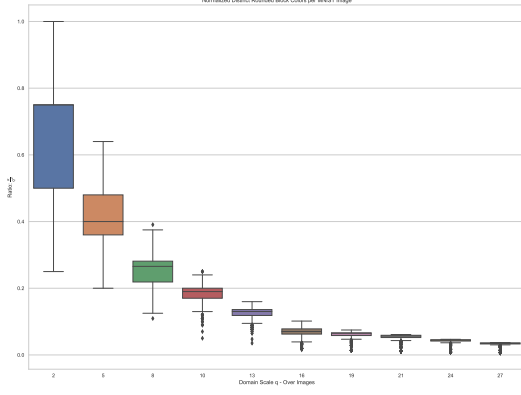


Figure 3: $\hbar = 10$.

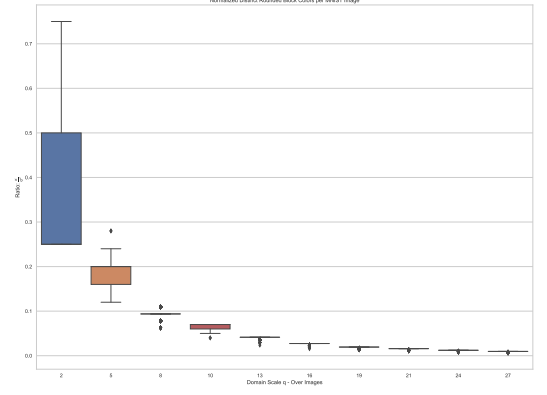


Figure 4: $\hbar = 50$.

Figure 5: Ratio of κ/q^2 of distinct greyscale colours for MNIST dataset relative to maximum possible number of distinct colours given by number of distinct superpixels/cells q^2 (y-axis). Here, \hbar is defined implicitly with 10 distinct grey-scale colours instead of 255 (default) for different values of q (x-axis).

Data: (uniformly) randomly sampling 5k MNIST images and counting the distinct number of repeated greyscale values after cell averaging for various values of q and \hbar .

Note: 1 means no repeated values (no/minimal symmetries in data), and a value of 0 means only repeated values (maximal symmetries in data).

considerations. In short, the next result guarantees that one symmetry (e.g. on colour in Figure 2 is repeated arbitrarily often; in the figure one instance of that repeated colour is the black colour.)

Proposition 3.1 (Arbitrarily Frequent Symmetries Are Unavoidable). *Let $q, \hbar, k \in \mathbb{N}_+$. If $f : [0, 1]^d \rightarrow [0, 1]$ is Lebesgue integrable then $f_{q, \hbar}$ is well-defined and $\#\{f_{q, \hbar}([0, 1]^d)\} \leq \hbar^d + 1$. Moreover, for any q large enough then there must exist a value $c \in \{f_{q, \hbar}([0, 1]^d)\}$ which is repeated at-least k times.*

The expressive power of this lower class is by no means limited, as the universal approximation capabilities of the function family in (9) can be established using arguments nearly identical to those in [113, 88, 101], which demonstrate the optimal approximation properties of ReLU MLPs; provided the parameters q , \hbar , and the coefficients of the square bump functions $\phi_{Q, \hbar} Q \in \mathcal{Q}$ are appropriately chosen⁶. Therefore, there is no loss in generality in henceforth assuming that the target function is, at-least approximately, of the coarsened form (9).

Our theory is based on the following abstraction of this pattern; summarized in Figures 2 and 7. Our theory concerns coarsened functions of the form (9); which are easily verified to themselves be universal (see Proposition D.1).

3.2 Formalizing Combinatorial Symmetries

We partition the domain $[0, 1]^d$ into cubes of side length $1/q$, for some integer scale q (the small boxes in Figure 7). Two cubes are identified as equivalent if they assign the same value at the centroid of each cube. More precisely, fix ambient dimensions $d, D \in \mathbb{N}_+$, a scale q , and consider the family of cubes

$$\mathcal{Q} \stackrel{\text{def.}}{=} \left\{ \prod_{k=1}^d \left[\frac{i_k}{q}, \frac{i_k + 1}{q} \right] : i_1, \dots, i_d \in [q] \right\}.$$

The mid-point \bar{Q} of any cube $Q = \prod_{i=1}^d [i_1/q, (i_1 + 1)/q] \in \mathcal{Q}$ is $\bar{Q} \stackrel{\text{def.}}{=} \left(\frac{2i_k + 1}{2q} \right)_{k=1}^d$. Fix a number of symmetries $\kappa \in \mathbb{N}_+$, out of a maximum number of possible symmetries $\kappa \leq 2^q$. A κ -combinatorial symmetry at scale q is any subjective map $\mathcal{S} : \mathcal{Q}_q \rightarrow [\kappa]$. Any such \mathcal{S} identified cubes by partitioning \mathcal{Q} into symmetry classes (illustrated by distinct colours in Figure 6); with each class indexed by $k \in [\kappa]$ is defined by

$$\mathcal{S}_k \stackrel{\text{def.}}{=} \{Q \in \mathcal{Q} : \mathcal{S}(Q) = k\}.$$

⁶These coarsening transformation $f \mapsto f_{q, \hbar}$ has the effect that it restricts the number of values the function in a class can take without limiting the expressivity of the class (see e.g. Proposition D.2).

Informally, a function is \mathcal{S} -symmetric if there is a repeating pattern in traceable by the marked centre points of each cube; which can be loosely thought of as an *aperiodic* multidimensional version of a sinusoidal pattern. The distinctness of each symmetry will be quantified by their distance, measured by a *separation level* $\epsilon > 0$.

Definition 3.1 (Symmetric Function). *Let $q, \kappa, d \in \mathbb{N}_+$ with $\kappa \leq q^d$ and fix a κ -symmetry at scale q , \mathcal{S} , and a separation level $\epsilon > 0$. A function $f : [0, 1]^d \rightarrow \mathbb{R}^D$ is (ϵ, \mathcal{S}) -symmetric at scale q , denoted $f \in S_{q, \epsilon}([0, 1]^d, \mathbb{R}^D)$ if*

- (i) **κ -Symmetries:** *For each $k \in [\kappa]$ and every $Q, \tilde{Q} \in \mathcal{S}_k$ we have $f(Q) = f(\tilde{Q})$,*
- (ii) **ϵ -Separation:** *If $k, \tilde{k} \in [\kappa]$ are distinct and $Q \in \mathcal{S}_k, \tilde{Q} \in \mathcal{S}_{\tilde{k}}$ then $\|f(Q) - f(\tilde{Q})\|_\infty \geq \epsilon$.*

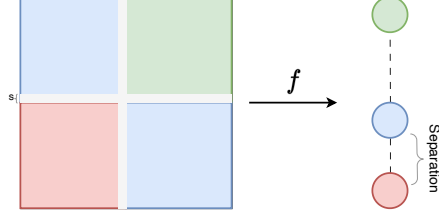


Figure 6: A function with a $(\epsilon, 3)$ -combinatorial symmetry at scale 2. Each symmetry class $\mathcal{S}_1, \mathcal{S}_2$, and \mathcal{S}_3 is illustrated by one of the three distinct colours. The values of the centre of each cube under the real-valued symmetric function f is illustrated by the coloured bubble lying on the (vertically placed) real line. The minimal distance between these bubbles is the function’s *separation level* (ϵ).

One may be tempted to wonder if there is any concrete link between the favourable combinatorial structure, quantified by these symmetries, and the classical favourable analytic structure given by a function admitting a certain number of continuous partial derivatives. The latter of which is classical both in learning [107, Chapter 2.7] and approximation theory of deep neural networks [55, 116, 75]. We close this section by showing that no such relationship exists.

Proposition 3.2 (Symmetries and Smoothness are Distinct). *Let $d, D, q, \kappa \in \mathbb{N}_+$ with $1 \leq \kappa \leq q^d$. For every smoothness level $s \in \mathbb{N}_+$ there exists a κ -symmetric function $f : [0, 1]^d \rightarrow \mathbb{R}^D$ at scale q with: all continuous partial derivatives up to order s but not up to order $s + 1$.*

Proof. We prove a more powerful version of this result in Appendix D. □

3.3 Similar Out-of-Distributional Tasks via Similarities

We consider two tasks to be similar or related if they share the same set of domain symmetries, as illustrated in Figure 7. In this figure, the first task (left) assigns three distinct values, represented by different colours, to four cubes, while the second task (right) assigns three different values to the same four cubes, maintaining the same pattern of repeated values; that is, in both cases, the top-left and bottom-right cubes share the same value. The number of these repeated values is referred to as the number of domain symmetries, denoted by κ . Identifying the locations of cubes with identical values is precisely the task that all but the final layer of our trained transformer learns to perform.

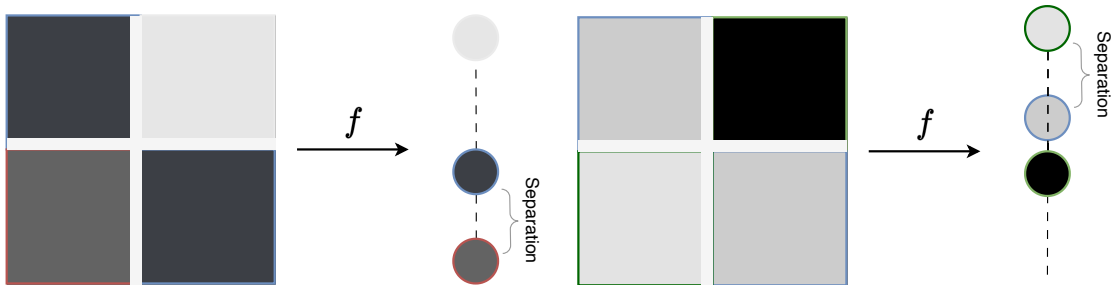


Figure 7: **Task Similarities via Symmetries:** While the new task (left) has very different values that then pre-training task (right), both are similar in the sense that they have the same underlying combinatorial symmetries structuring the their *domain not their range* (function values given the symmetries on their domain).

A task $\tau \stackrel{\text{def.}}{=} (f, \mathbb{P}_X, \mathbb{P}_\varepsilon)$ is defined by a “signal” meaning, a Borel function $f : [0, 1]^d \rightarrow \mathbb{R}^D$, to be learned, a *sampling distribution* \mathbb{P}_X on $[0, 1]^d$ therefrom our samples are drawn, and a *measurement noise* distribution \mathbb{P}_ε on \mathbb{R}^D . We assume on the following on the measurement noise:

Assumption 3.1. *There is some $C \geq 0$ and $\sigma > 0$ such that \mathbb{P}_ε is centred (C, σ^2) -Sub-Gaussian.*

The task distribution is the distribution of the any *training set* from the task τ , by which we mean:

Definition 3.2 (Task Training Set). *Let $\tau \stackrel{\text{def.}}{=} (f, \mathbb{P}_X, \mathbb{P}_\varepsilon)$ be a task. A τ -training set is a (non-empty finite) set of random variables $\{(X_n, Y_n)\}_{n=1}^N$ in \mathbb{R}^{d+D} where: $\{X_n, \varepsilon_n\}_{n=1}^N$ are independent, $X_1 \sim \dots \sim X_N$ are i.i.d. with law \mathbb{P}_X , and $\varepsilon_1 \sim \dots \sim \varepsilon_N$ are i.i.d. with law \mathbb{P}_ε .*

We may formalize figure 7 as follows.

Definition 3.3 (Task Similarity: \mathcal{S} -Symmetric Task). *A task $\tau = (f, \mathbb{P}_X, \mathbb{P}_\varepsilon)$ is $(\varepsilon, \mathcal{S})$ -symmetric at scale q if \mathcal{S} is a κ -symmetry at scale q and f is ε -separated. We say another task $\tilde{\tau} = (\tilde{f}, \mathbb{P}_X, \mathbb{P}_\varepsilon)$ is similar to τ at scale q if \tilde{f} is $(\tilde{\varepsilon}, \mathcal{S})$ -symmetric for any $\tilde{\varepsilon} > 0$; in which case, we write $\tilde{\tau} \sim \tau$.*

Tasks are understood as being similar, not (necessarily) if the signal f have similar same values, but if they have the same set of symmetries. One possible answer to this question, illustrated by Figure 7, is given by them sharing the same set of (domain) symmetries rather than having similar output values.

3.4 Further Notation

We denote the outputs of Algorithms 1, 2, and 3 (defined below in Section 5) by Algo- i for $i = 1, 2, 3$ respectively. We say β solves the linear regression problem for a dataset $\mathcal{D} \stackrel{\text{def.}}{=} \{(X_n, Y_n)\}_{n=1}^{N'}$ if

$$\beta_{\text{OLS}; \mathbb{X}, \mathbb{Y}} \stackrel{\text{def.}}{=} (\mathbb{X}^\top \mathbb{X})^\dagger \mathbb{X}^\top \mathbb{Y} \quad (10)$$

where $\mathbb{X} \stackrel{\text{def.}}{=} (X_1, \dots, X_{N'})^\top$, $\mathbb{Y} \stackrel{\text{def.}}{=} (Y_1, \dots, Y_{N'})^\top$, and A^\dagger denotes the Moore-Penrose pseudo-inverse of a matrix A . If \mathbb{Q} is a probability measure on $\mathcal{P}([0, 1]^d)$, we denote the *essential-supremum* of a Borel function $f : [0, 1]^d \rightarrow \mathbb{R}$ by

$$\text{ess-sup}_{\mathbb{Q}} f(x) \stackrel{\text{def.}}{=} \inf U_f^{\text{ess}} = \{a \in \mathbb{R} : \mathbb{Q}(f^{-1}(a, \infty)) = 0\}.$$

We now present our training algorithm.

4 The Training Algorithm

Intuition Behind Training Algorithm - In the context of grayscale images: The trained transformer model in Figure 1 *reconstructs the missing pixel colours in an image* as follows. First, it’s trained attention mechanism groups together every pixel with a (sufficiently similar) grayscale colour, and represents the group by a single “representative” pixel. Next, it learns to interpolate/memorize the colour values for every observed superpixel representative using a two-layer ReLU MLP with an additional random linear projector layer (unactivated and untrained), followed by an affine linear layer trained with standard (unregularized) linear regression.

The result is a model that routes any new input pixel to its nearest cluster, i.e., the one with the most similar greyscale value, and assigns it the same colour as that cluster’s representative pixel. Our preprocessing step (Algorithm 1) and clustering/attention-training step (Algorithm 2), both subroutines of our training algorithm, can (approximately) recover the correct colour for each superpixel group and efficiently encode it into the keys and values matrices, which then perform the same extraction on out-of-sample inputs. Our results also show that the trained attention layer and the MLP block serve different roles in our transformer; namely, the first *reasons*, in that, it maps new data to previously observed simplified representation, while the MLP only efficiently *interpolates*.

The Base Assumption - Sampling, Feature, and Quantization Size: We now breakdown the subroutines of our training Algorithm, and explain the properties of each sub-Algorithm. We henceforth operate under the following set of assumptions.

Setting 4.1. *Let $d, q, \kappa, N, F \in \mathbb{N}_+$, with $\kappa \leq q^d$, and let $\varepsilon > 0$. Fix a κ -symmetry \mathcal{S} at scale q . All target functions $f : \mathbb{R}^d \rightarrow \mathbb{R}^D$ are L -Lipschitz for some $L \geq 0$.*

Our main results hold if the sample size (N), the scale (q), and the deep features (F) are large enough; by which we mean:

Assumption 4.1 (N , q , and F are Large Enough). *In Setting 4.1, we require:*

$$(i) \ N \geq \left\lceil \frac{1}{4p^*} \sqrt{\log\left(\frac{Q^*}{\delta}\right) \left(\frac{64\bar{\sigma}^2 q^2 \ln\left(\frac{Q^*}{2\delta}\right)}{L^2 d} + \log\left(\frac{Q^*}{\delta}\right) \right)} + \frac{8\bar{\sigma}^2 q^2 \ln\left(\frac{Q^*}{2\delta}\right)}{L^2 d} + \frac{\log\left(\frac{Q^*}{\delta}\right)}{4p^*} \right\rceil$$

$$(ii) \ q \geq L/\varepsilon$$

$$(iii) \ F > \kappa^{\mathcal{O}(\alpha)} \text{ and } F \geq \Delta^{\mathcal{O}(1+\alpha)}$$

where the task complexity at scale q is $\Delta \stackrel{\text{def.}}{=} \kappa^q$ (for absolute constants $C_1, \alpha > 0$ as in Theorem 5.1). Finally, we ask that $\mathbb{P}_X \in \mathcal{P}([0, 1]^d)$ is non-atomic⁷

The full-explicit version of Setting 4.1 and Assumption 4.1 is given in the appendix A; without the L -Lipschitz assumption and only requiring uniform continuity.

4.1 Pre-Processing: Denoising Algorithm

The following denoising algorithm builds a small virtual, or surrogate, dataset from any noisy dataset with the property that: given enough training samples, the new virtual dataset, a smaller dataset, roughly contains no noise.

Algorithm 1 Denoise and Compress: *From Large Noisy Dataset to Clean Small Dataset.*

Require: Dataset $\mathcal{D} \stackrel{\text{def.}}{=} \{(x_n, y_n)\}_{n=1}^N$.

$\mathcal{D}^* \leftarrow \emptyset$

for $Q \in \mathcal{Q}$ **do** $\mathcal{D}_Q \leftarrow \{(\mathbf{x}, \mathbf{y}) : \mathbf{x} \in Q\}$

if $\mathcal{D}_Q \neq \emptyset$ **then**

$$\mathbf{y} \leftarrow \frac{1}{N_Q} \sum_{(x, y) \in \mathcal{D}_Q} y$$

▷Average Cube Value

$$\mathcal{D}^* \leftarrow \mathcal{D}^* \cup \{(\bar{Q}, \mathbf{y})\}$$

▷Add new Data-point

$$\mathcal{D} \leftarrow \mathcal{D} \setminus \mathcal{D}_Q$$

▷Remove Redundant Data

end if

end for

return \mathcal{D}^*

▷Return Distilled Dataset

Here, $N_Q \stackrel{\text{def.}}{=} \#\mathcal{D}_Q$; i.e. the number of data-points in cube Q .

The following result shows that roughly $\mathcal{O}(Q^* \log Q^*)$ training samples suffice to de-noise the dataset and observe at least one representative sample in each cube at scale q , where Q^* denotes the covering number of the support of the sampling distribution \mathbb{P}_X by ℓ^∞ -balls of radius $1/q$. We require only *logarithmically* more samples than the number of such cubes covering the support of \mathbb{P}_X . When the support has doubling dimension $0 < \bar{d} \leq d$, Q^* scales as $q^{\bar{d}}$. In the plausible worst case; e.g., when \mathbb{P}_X is uniform on the cube $[0, 1]^d$ — Q^* grows exponentially as q^d .

Remark 4.1. *We remind the reader that the supremum over an emptyset is defined as being positive infinity.*

Proposition 4.1 (Recovery for Lipschitz Functions with Low-Dimensional Data-Generating Distribution). *Under Setting 4.1, let $L \geq 0$, fix $q \in \mathbb{N}_+$, denote the number of cubes with mass is $1 \leq Q^* \stackrel{\text{def.}}{=} \#(\text{supp}(\mathbb{P}_X) \leq q^d$ and the minimum probability of sampling any supported cube by $p^* = \min_{Q \in \mathcal{Q}, \mathbb{P}_X(Q) > 0} \mathbb{P}_X(Q)$. If f is L -Lipschitz then, for any $\delta > 0$ small enough, with a scale of $q \geq \frac{L}{\varepsilon}$ if the sample size N is at least*

$$N \geq \left\lceil \frac{1}{4p^*} \sqrt{\log\left(\frac{Q^*}{\delta}\right) \left(\frac{64\bar{\sigma}^2 q^2 \ln\left(\frac{Q^*}{2\delta}\right)}{L^2 d} + \log\left(\frac{Q^*}{\delta}\right) \right)} + \frac{8\bar{\sigma}^2 q^2 \ln\left(\frac{Q^*}{2\delta}\right)}{L^2 d} + \frac{\log\left(\frac{Q^*}{\delta}\right)}{4p^*} \right\rceil \quad (11)$$

then, we have

$$\mathbb{P}\left(\max_{Q \in \mathcal{Q}_p} \left\| f(\bar{Q}) - \frac{1}{N_Q} \sum_{(X, Y) \in Q} Y_Q \right\| \leq \varepsilon \right) \geq 1 - \delta. \quad (12)$$

⁷That is, there no Borel set A such that $\mathbb{P}_X(A) > 0$ and all measurable subsets $B \subseteq A$ have the same mass; i.e. $\mathbb{P}_X(B) = \mathbb{P}_X(A)$. E.g. 1) any measure which is absolutely continuous with respect to the uniform measure on $[0, 1]^d$ is non-atomic and 2) any “reasonable” measure supported on a lower-dimensional space, namely any Ahlfors \bar{d} -regular measure for $0 < \bar{d} \leq d$, is non-atomic (see e.g. [8, Equation (1.1)] for definitions).

Proof. See Appendix B.1 for a proof of a more technical formulation when f is only (uniformly) continuous. \square

4.2 Pre-Training: Domain Learning

Algorithm 2 Initialize Keys and Values

Require: Dataset $\mathcal{D} \stackrel{\text{def.}}{=} \{(x_n, y_n)\}_{n=1}^N$, tolerance $\varepsilon > 0$.

$\mathcal{C} \leftarrow \emptyset$

▷Initialize: Clusters

$\mathcal{D}^* \leftarrow \emptyset$

▷Initialize: Compressed training data

while $\mathcal{D} \neq \emptyset$ **do**

$(\mathbf{x}, \mathbf{y}) \leftarrow \text{Unif}(\mathcal{D})$

▷Pick un-clustered reference point randomly

$\mathcal{C}_{(\mathbf{x}, \mathbf{y})} \leftarrow \{(x, y) \in \mathcal{D} : \|y - \mathbf{y}\| < \varepsilon/8\}$

▷Create cluster around point

$\mathcal{D} \leftarrow \mathcal{D} \setminus \mathcal{C}_{(\mathbf{x}, \mathbf{y})}$

▷Remove cluster from set of unclustered points

$\mathcal{C} \leftarrow \mathcal{C} \cup \mathcal{C}_{(\mathbf{x}, \mathbf{y})}$

▷Append new cluster to collection of clusters

$\mathcal{D}^* \leftarrow \mathcal{D}^* \cup (\mathbf{x}, \mathbf{y})$

▷Append representative point to compressed training set

end while

$K \leftarrow (x_n)_{n=1}^N$

▷Write $d \times N$ keys matrix

$V \leftarrow \left(\frac{1}{\sqrt{d}}x\right)_{x \in \mathcal{D}^*} (I_{x_n \in c})_{c \in \mathcal{C}, n=1}^N$

▷Write $d \times N$ -dimensional values matrix

return K, V , and \mathcal{C}

Having run Algorithm 2, we would have successfully extracted enough structure from our denoised training set to construct a light interpolator *if* the training data has enough structure. Our next result shows that the max-temperature attention mechanism correctly produced by Algorithm 2 correctly routes any input in \mathbb{R}^d to the maximal cluster $c \in \mathcal{C}$ of cubes whose centroid is mapped to the same value; , omitting a negligible “bad set”.

Proposition 4.2 (Feature Encoding Properties of Attention Initialized by Algorithm 2). *In the setting of Lemma B.2, fix a failure probability $0 < \delta \leq 1$ and let N satisfy (29). Fix $\varepsilon > 0$ and suppose that the scale q satisfies*

$$\frac{2^5 \sqrt{d}}{L\varepsilon} \leq q \quad (13)$$

and suppose that $f(\{\bar{Q}\}_{Q \in \mathcal{Q}^})$ is ε -separated. Let $\mathcal{C}, \mathcal{D}, V$ and K be as in Algorithm 2 with input $\mathcal{D} = \mathcal{D}^* = \{(x_c, y_c)\}_{c \in \mathcal{C}}$ from Algorithm 1, and suppose that MLP’s hidden feature dimension F satisfies*

$$\Delta^{C^2(1+\alpha)} \leq F \quad (14)$$

where the task complexity at scale q is $\Delta \stackrel{\text{def.}}{=} \kappa^q$ and $\kappa \stackrel{\text{def.}}{=} \#\mathcal{C}$. Then, the following holds with probability at-least $1 - \delta$ on the draw of $\{(X_n, Y_n)\}_{n=1}^N$:

(i) **Cluster identifiability:** *For all $x \in \mathcal{G}$ and all $c \in \mathcal{C}$*

$$\text{Attn}(x|K, V) = \frac{1}{\sqrt{d}}x_c \Leftrightarrow x \in \bigcup_{Q \in c} Q \text{ and } (\forall Q \in c) f(\bar{Q}) = y_c$$

(ii) **Separation:** $C \sqrt{\frac{(1+\alpha) \log \#\mathcal{C}}{\log F}} \leq \min_{\substack{x, \tilde{x} \in \mathcal{D}^* \\ x \neq \tilde{x}}} \left\| \frac{1}{\sqrt{d}}x - \frac{1}{\sqrt{d}}\tilde{x} \right\|_2,$

(iii) **Norm-Boundedness:** $\max_{x \in \mathcal{D}^*} \frac{\|x\|_2}{\sqrt{d}} \leq 2,$

where $\mathcal{G} \stackrel{\text{def.}}{=} \mathbb{R}^d \setminus \bigcup_{c \in \mathcal{C}, Q \in c} \partial Q$ and $C > 0$ is an absolute constant.

4.2.1 Well-Conditioned Deep Feature Matrix (Encoder MLP at Random Initialization)

We now specify the initialization scheme used for the weights and biases of our 3-layer MLP encoder. Our procedure largely follows standard random initialization protocols, with a mild but deliberate modification: we adjust the variance of the random weight matrices and choose non-random biases, following insights from [110]. The MLP layers

are primarily responsible for constructing a feature/design matrix from the outputs of the single-head attention mechanism. This design ensures that the resulting ridgeless regression problem is well-posed with overwhelming probability; that is, interpolation of the training data is likely to be possible with high probability.

Algorithm 3 Initialize: MLP Encoder

Require: Width parameters $d, F, C \in \mathbb{N}_+$

Require: Widths $d_0 \leftarrow d, d_1 \leftarrow F, d_2 \leftarrow F, d_3 \leftarrow C$

$$p^{(1)} \leftarrow \frac{C \log^2(2NF)}{N^{-2(1+\alpha)} F}, p^{(2)} \leftarrow \frac{1}{\sqrt{F}}$$

for $i = 1, 2$ **do**

 Generate: $B^{(i)}$ a $d_i \times d_{i-1} N(0, 1)$ Random Matrix

$$b^{(i)} \leftarrow \text{Solve: } p^{(i)} = (b^{(i)})^2 (1 - \Phi_{CDF}(b^{(i)})) - \frac{b^{(i)}}{\sqrt{2\pi}} e^{-\frac{(b^{(i)})^2}{2}}$$

$$\mathcal{L}^{(i)} \leftarrow \text{ReLU}(B^{(i)} \cdot + b^{(i)})$$

end for

Generate: Π a $C \times F N(0, 1/\sqrt{C-1})$ Random Matrix

$$\mathcal{E} \stackrel{\text{def.}}{=} \Pi \mathcal{L}^{(2)} \circ \mathcal{L}^{(1)}$$

return \mathcal{E}

▷Initialize Hidden Layers

▷Initialize Unactivated Layer

▷Return Initialized MLP Encoder

Proposition 4.3 (Well-Conditioning of Deep Random Feature Matrix: MLP Encoder at Initialization). *There is an absolute constants $C, \tilde{C}, \alpha > 0$ such that: for any, sufficiently large, integers $F, \kappa \in \mathbb{N}$ such that*

$$F > \kappa^{5(1+\alpha)} \quad (15)$$

and any features $\{u_k\}_{k=1}^\kappa$

$$\|u_k\|_2 \in [0, 2], \forall k = 1, \dots, \kappa \text{ and } \|u_k - u_{\tilde{k}}\|_2 \geq C \sqrt{\frac{(1+\alpha) \log(\kappa)}{\log(F)}}, \forall k \neq \tilde{k} \quad (16)$$

if the MLP encoder \mathcal{E} is (randomly) initialized using Algorithm 3 then: the smallest singular value $s_{\min}(\mathbb{X})$ of the deep feature matrix

$$\mathbb{X} \stackrel{\text{def.}}{=} 1_\kappa \oplus (\mathcal{E}(u_1), \dots, \mathcal{E}(u_\kappa)) \in \mathbb{R}^{\kappa \times \kappa}$$

satisfies the well-conditioning guarantee

$$s_{\min}(\mathbb{X}) \geq \left(\frac{1}{2} - \frac{C_2(1+\alpha) \log^2 N}{N^{(3+\alpha)/2}} \right) (N^{2+\alpha/2} - C) \quad (17)$$

and the boundedness guarantee

$$s_{\max}(\mathbb{X}_\Psi) \leq \sqrt{\left(C + 2N \log F + \log^2(2F^2) \right)^2 \left(\frac{1}{\sqrt{k}} + \frac{C}{\sqrt{F}} \right)^2 + N^2} \quad (18)$$

holds with probability at least $1 - 2e^{-N} - 2N^{-3-20(1+\alpha)}$ over the draw of $B^{(1)}, B^{(2)}$, and Π ; where $s_{\min}(\mathbb{X})$ is the smallest singular value of the random matrix \mathbb{X} .

5 Main Results

We now present our main result, which shows that when our the transformer network in Figure 1 is trained using Algorithm 1, 2, 3 then it can uniformly approximate the ground truth function even from noising training data. This is our main learning-theoretic universal approximation theorem.

Theorem 5.1 (Algorithmic Universal Approximation from Noising Training Data). *If q, N, F satisfy Assumption A.1 then: for any $\mathcal{D}_\tau \stackrel{\text{def.}}{=} \{(X_n, Y_n)\}_{n=1}^N$ be a τ -training set from a $(\varepsilon, \mathcal{S})$ -symmetric task τ : let $\mathcal{D}_\tau^\star \stackrel{\text{def.}}{=} \{(x_c, y_c)\}_{c=1}^\kappa \stackrel{\text{def.}}{=} \text{Algo-1}(\mathcal{D}_\tau), (V, K) \stackrel{\text{def.}}{=} \text{Algo-2}(\mathcal{D}^\star), \mathcal{E} \stackrel{\text{def.}}{=} \text{Algo-3}(d, F, \kappa)$, and respectively consider the $\kappa \times \kappa$ induced (random) deep design matrix and $D \times \kappa$ -regression targets*

$$\mathbb{X} \stackrel{\text{def.}}{=} 1_\kappa \oplus (\mathcal{E}(x_c))_{c=1}^\kappa \text{ and } \mathbb{Y} \stackrel{\text{def.}}{=} (y_c)_{c=1}^\kappa. \quad (19)$$

Then, \mathbb{X} is **invertible** and the following linear regression problem has a **unique solution** $\beta_{\text{OLS}:\mathbb{X},\mathbb{Y}}$ with $\beta \in \mathbb{R}^{D \times \kappa}$

$$\beta \mathbb{X} = \mathbb{Y} \quad (20)$$

given by (10), with probability at-least $1 - \delta(\kappa, N)$ (over the draw of \mathcal{D}_τ and the random matrices $B^{(1)}, B^{(2)}$, and Π in Algorithm 3); for absolute constants $\alpha, C_1, C_2 > 0$ satisfying $\delta(\kappa, N) \stackrel{\text{def.}}{=} (1 - \frac{1}{N})((\frac{1}{2} - \frac{C_2(1+\alpha)\log^2(\kappa)}{\kappa^{(3+\alpha)/2}})(\kappa^{2+\alpha/2} - C_1))$.

Moreover, the following regularity guarantee holds

$$\|\beta_{\text{OLS}:\mathbb{X},\mathbb{Y}}\|_{\text{op}} \lesssim \frac{\sqrt{D} \left(\log F \left(\frac{1}{\sqrt{\kappa}} + \frac{1}{\sqrt{F}} \right) + 1 \right)}{\kappa^{3+\alpha-1/2}}. \quad (21)$$

We now demonstrate that the cost of out-of-distribution learning, via fine-tuning our transformer models pretrained with our proposed algorithm, scales favourably with the number of combinatorial symmetries present in the training data. Importantly, the following theorem also applies in the in-distribution setting, i.e., to the original training dataset, and thereby establishes each of the claims summarized in Table 1.

Theorem 5.2 (Scalable Fine-Tuning). *In the setting of Theorem 5.1, conditioned on the success of (20): For training set of training data $\mathcal{D}_{\tilde{\tau}} \stackrel{\text{def.}}{=} \{(\tilde{X}_n, \tilde{Y}_n)\}_{n=1}^{\tilde{N}}$ \mathcal{S} -symmetric task $\tilde{\tau} \stackrel{\text{def.}}{=} (\tilde{f}, \tilde{\mathbb{P}}_X, \tilde{\mathbb{P}}_\varepsilon)$ for which $\tau \sim \tilde{\tau}$ at scale q . Let $\mathcal{D}_{\tilde{\tau}}^* \stackrel{\text{def.}}{=} \text{Algo-1}(\mathcal{D}_{\tilde{\tau}}) = \{(\tilde{x}_c, \tilde{y}_c)\}_{c=1}^{\kappa}$, and set $\beta_{\text{OLS}:\mathcal{D}_{\tilde{\tau}}^*}$ as in (10). Fix a failure probability $0 < \delta \leq 1$. If \tilde{N} satisfies the lower-bound (11) then, with probability at-least $1 - \delta$ over the draw of $\mathcal{D}_{\tilde{\tau}}$ the $\beta_{\text{OLS}:\mathcal{D}_{\tilde{\tau}}^*}$ is the unique solution to the OLS problem*

$$\beta \mathbb{X} = \tilde{\mathbb{Y}} \text{ where } \tilde{\mathbb{Y}}^\top = (\tilde{y}_c)_{c=1}^{\kappa} \quad (22)$$

and the following uniform approximation

$$\text{ess-sup}_{x \in [0,1]^d} \|\tilde{f}(x) - \beta_{\text{OLS}:\mathcal{D}_{\tilde{\tau}}^*} \mathcal{E}(x)\| \lesssim \omega(\sqrt{d}/q) + \frac{1}{q}. \quad (23)$$

Proof. The proofs of Theorems 5.1 and 5.2 is given in Appendix B.3. \square

Which, and How Many, Parameters are Trained? We emphasize that only the parameters in our network's *initial* clustering attention layer \mathcal{E} and those in its *final* linear output/readout layer $\beta \cdot$, c.f. (3), are trained by Algorithms 1, 2, and 3. All other parameters are randomized and frozen. A careful parameter count shows that, when the target function f is Lipschitz, only $\mathcal{O}(\varepsilon^{-d})$ parameters are trained. Consequently, our networks achieve the minimax-optimal rate, c.f. [101, Theorem 2.4], matching the rates established in the minimax-optimal universal approximation theorems [114, Theorem 2] and [101, Theorem 1.1].

5.1 How Many Oracle Samples Are Needed for Algorithmic Approximation?

One may wonder how many samples are needed if they operate under the context of a universal approximation theorem, where one can effectively *query and oracle* and obtain noiseless. The following result shows that, as one may intuit, the number of oracle (ideal) samples is no more than the number of symmetries κ in the ground truth function. We emphasize that *Algorithm 1 is not needed when oracle samples are available*.

Proposition 5.1 (Sample Complexity - Oracle Samples). *In the setting of Theorem 5.1, conditioned on the success of (20). Let $\tilde{f} : \mathbb{R}^d \rightarrow \mathbb{R}^D$ be \mathcal{S} -symmetric and for every symmetry $c \in [\kappa]$ let $x_c = \tilde{Q}$ for some $Q \in c$ and $y_c = \tilde{f}(x_c)$. Then, there exists a **unique** solution $\tilde{\beta}$ to the OLS problem*

$$\beta \mathbb{X} = \tilde{\mathbb{Y}} \stackrel{\text{def.}}{=} (y_1, \dots, y_\kappa)^\top$$

and the fine-tuned transformer $\tilde{\beta} \mathcal{E}(\cdot)$ satisfies

$$\sup_{x \in [0,1]^d} \|\tilde{f}(x) - \tilde{\beta} \mathcal{E}(x)\| \leq \omega\left(\frac{\sqrt{d}}{\kappa}\right).$$

Proof. Obtained by tweaking the proof of Theorem 5.2. \square

5.2 Sub-Linear Samples Complexity is Achievable on Similar OOD Regression Tasks

We conclude our analysis by showing that if enough symmetries are present in a similar OOD task, then arbitrarily **fast sub-linear** learning rates are achievable.

Corollary 5.1 (Sub-linear Learning Rates). *In the setting of Proposition 5.1, if $\tilde{f} : \mathbb{R}^d \rightarrow \mathbb{R}^D$ be (L, α) -Hölder for some $L \geq 0$ and some $0 < \alpha \leq 1$ and if exist $C > 0$ and $1 > r > 0$ such that for every $q \in \mathbb{N}_+$*

$$\frac{\ln(\kappa/C)}{\ln(q)} \leq r \text{ and } r < \frac{1}{\alpha} \quad (24)$$

then the fine-tuned transformer $\tilde{\beta}\mathcal{E}$ satisfies

$$\sup_{x \in [0,1]^d} \|\tilde{f}(x) - \tilde{\beta}\mathcal{E}(x)\| \lesssim \frac{1}{\sqrt[r]{N}} < \frac{1}{\tilde{N}}$$

where \lesssim hides the constant $C_{L,\alpha,d} \stackrel{\text{def.}}{=} \sqrt[\alpha]{L} \sqrt[2\alpha]{d} > 0$.

Proof. Direct consequence of Corollary (24), when κ scales like (24). \square

6 Discussion

We briefly unpack each element introduced in our paper and how they operate.

6.1 Explaining Our Trained Transformers

We summarize the key structural features of the transformers produced by our stylized training algorithm, as illustrated in Figure 1. Our aim is to clarify how these models learn and predict by making explicit the roles played by their internal components. Broadly speaking, the trained models decompose into three blocks, each performing a distinct function, following an initial “denoising and summarization data-preprocessing step”.

Phase 1 - Clustering and Efficient Representation in the Attention Mechanism The first component is the **clustering phase**, implemented by the attention mechanism. In this stage, the max-temperature attention learns to perform a bi-level clustering of the domain: (1) grouping nearby points in the input space into the same cluster, (2) grouping points whose target values are similar⁸, and (3) assigning each cluster a single representative point in the transformer.

In the trained model, the **keys** matrix contains, as its columns, one representative for every quantized cube of side length $\frac{1}{q}$, while the **values** matrix stores the representative point associated with each cluster.

At inference time, given a new test point x , the attention mechanism executes clustering and representative selection as follows: the distance from x to each column of the keys matrix is computed to determine the nearest cube, the resulting alignment scores are processed by the softmax function, and the corresponding column of the values matrix—representing the cluster’s representative point—is returned.

Remark 6.1 (Is Attention needed?). *One could, in principle, replace the attention mechanism with a sufficiently complex ReLU MLP of depth $\mathcal{O}(d)$ and width $\mathcal{O}(q^d)$, following the constructions in [89, Lemmata 5.11 and 5.3]. However, such a network would be far from conducive to a realistic algorithmic implementation. Thus, while ReLU MLPs can, in theory, compute the transformers constructed in our main result (Theorem 5.1), it is not clear that they can do so in a practically implementable way—an obstacle that does not arise for transformers.*

We therefore speculate, cautiously, that one of the principal advantages transformers may enjoy over their ReLU MLP counterparts is their amenability to efficient training. This conjecture is further supported by the recent results of [65] showing that the in-context representation power of ReLU MLPs and transformers are, in theory, the same.

⁸One can interpret this as quantizing similarly to the quantization in Riemannian sums, in Riemann integration, and simple functions in Lebesgue integration, respectively; which respectively summarize the domain and range of the functions they are handling. Here, we find it advantageous to simultaneously perform both such summarizations. Note, classical optimal approximation theorems in the Lipschitz class, e.g. [113, 101, 52], *only* quantize based on the domain since they do not consider not making use of any symmetry structure to simplify down-stream fine-tuning.

Phase 2 - Separation: The second **separation phase** processes the cluster representatives through a randomized, frozen three-layer MLP: the first two layers use ReLU activations, while the final layer remains unactivated. This stage serves to organize each cluster’s representative point as orthogonal vectors in representation space of minimal dimension. Importantly, this is possible because the stored values are always sufficiently well-separated for such a separation to be possible; a feature not shared by many ReLU MLP memorization results; cf. [110].

Phase 3 - Linear Regression on Deep Features: The final **linear regression phase** leverages the well-conditioned design matrix to guarantee interpolation: the trained linear layer achieves zero training error, while the spectral bounds on the design matrix ensure that the learned mapping possesses a high degree of Lipschitz regularity.

Importantly, the size of this final layer scales with the number of symmetries of the target function rather than with the approximation error. Consequently, when the target function exhibits sufficient structure, this phase can be retrained without succumbing to the curse of dimensionality. A property not shared by state-of-the-art universal approximation theorems (even assuming ideal data); cf. [101, 52].

6.2 The role of Algorithm 1: Creation of a Denoised Virtual Dataset

Broadly speaking, Algorithm 1 *de-noises* and compresses the training data, into a fixed number of “purified” representative paired samples. Its objective is to *recover* the underlying function by removing the noisy labels and correct the input sample locations for ideal points in the input space.

It is worth noting that this algorithm shares a key similarity with learning-theoretic *compression schemes* (e.g., [73, 42, 82]), in the sense that both our approach and traditional compression schemes produce a small dataset of fixed size for learning. However, it also has a very large key difference from such schemes: namely it does not return a subset of the original training data but rather, it returns a new *virtual dataset* which contains more “directly usable” information about the ground truth function.

For these reasons, we expect that Algorithm 1 is of independent interest beyond our training scheme and that it, or a suitable variation thereof, can likely be incorporated into a wide range of deep learning pipelines.

Remark 6.2. *We note that Algorithm 1 can be omitted if one can directly query specific noiseless samples from the target function, as is possible in certain optimal approximation theorems [52]. Such results are sometimes referred to as practical existence theorems [17, 18, 43]. However, most standard deep learning pipelines make little to no attempt to automatically improve data quality before training. Our analysis shows that performing this step via Algorithm 1 enables approximate reconstruction of the ground-truth function, even from noisy samples.*

6.3 What’s Left: Our Customized Training Algorithm vs. Gradient Descent

As indicated in Table 1, our analysis leaves one outstanding step when closing the gap between machine learning theory and practice. Namely, quantifying the networks obtained from our training algorithm and those obtained with variants of stochastic gradient descent.

We offer some one dimensional plots showcasing the behaviour of our algorithm against the same models trained with SGD in hopes of speculating how this last step could be addressed in future research. We *stress* that this investigation is not intended to demonstrate scalability or to position our algorithms as practical replacements for optimizers like SGD or ADAM. Instead, we aim to establish two points: (1) Algorithms 1, 2, and 3 are implementable and do not exist solely within a theoretical vacuum; and (2) they yield networks that display both familiar and novel behaviours relative to those trained with classical methods. To make these comparisons transparent and visually meaningful, we restrict our focus to the one-dimensional Euclidean domain $[0, 1]$, where the learned functions can be directly plotted and inspected.

Comparison with Trained Layer MLPs and Random Feature Models Frequency bias is a known known phenomenon where neural networks learn low frequency signals earlier than the high frequency one [83, 81], hence the network only learns such details in later epochs. However, algorithm 2 clusters the data and mitigate this problem, allowing the model to learn high frequency signals early on, see fig. 9 and fig. 10 for details.

100 Epochs (Partial Training Benchmarks)

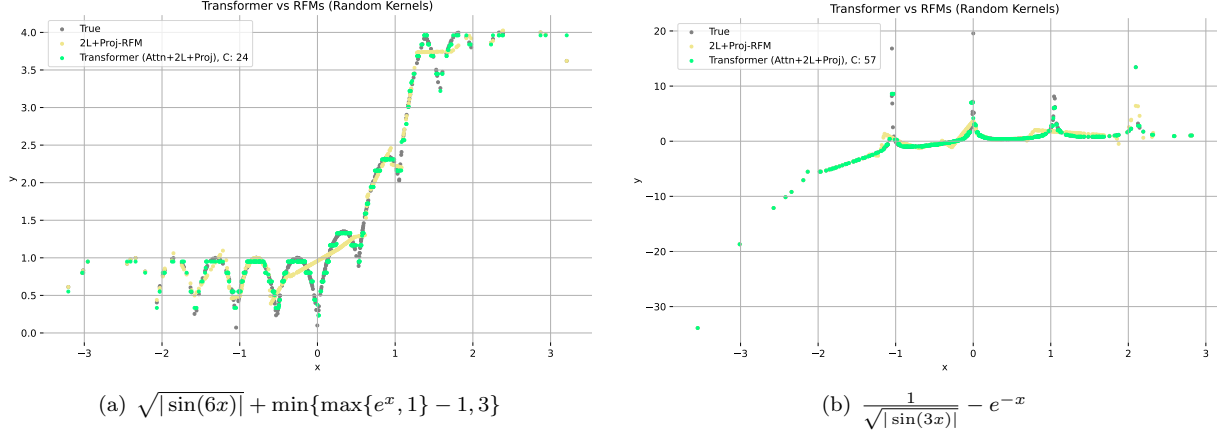


Figure 8: A comparison between random feature models (RFMs: 1, 2 activated layers, as well as 2 activated learns and one unactivated random projection layer) against a transformer studied herein.

Conclusion: Attention improves detail (high fidelity patterns) capturing and while RFMs only capture general trends (low-fidelity patterns).

The domain adaptation effect of pre-training attention, even without appealing to any end-to-end (stochastic) gradient descent procedure, is a non-trivial advantage of attention-based models over their classical “attention-less” MLP counterparts. Interestingly, in many cases, only training the first and last layers of our transformer with two activated MLP layers following one attention head (Transformer) consistently outperforms its classical MLP counterpart trained *with* (stochastic) gradient descent (MLP Trained).

100 Epochs (Partial Training Benchmarks)

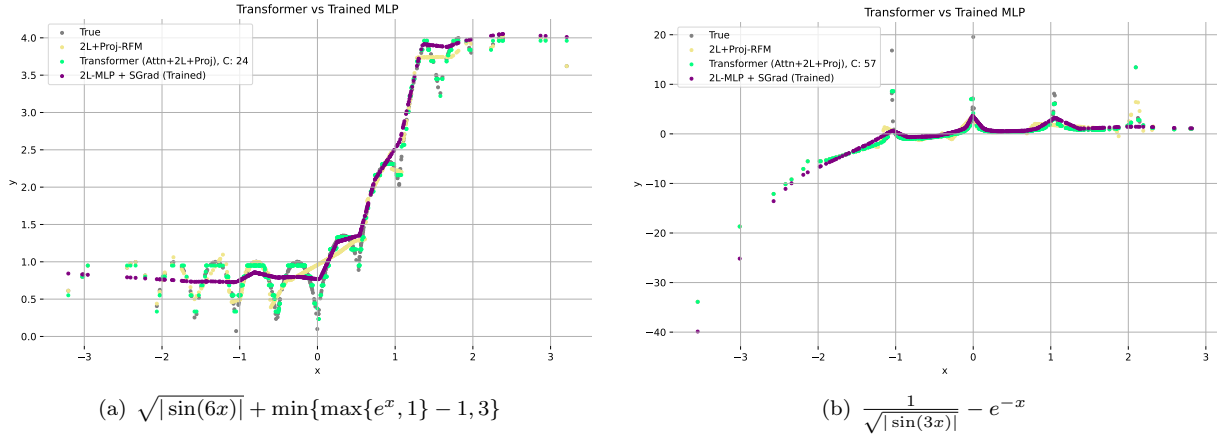


Figure 9: Comparison: A typical (100 epochs) trained (ADAM) 2-layer MLP vs. B) randomly initialized transformer with one attention head and 2 activated MLP layers and one trained final MLP output layer.

Our examples across two challenging functions, illustrated in Figure 8, have little-to-no classically recognizable or tame patterns; the first is aperiodic oscillatory, and the second has periodic singularities. However, as each function is non-injective, one can readily see that it possesses some complicated symmetries. Figure 9 illustrates that the attention mechanism can capture high-fidelity details of the target task even before gradient descent training begins. These fine-grained features—such as sharp spikes and singularities—are typically learned only in the later stages of (stochastic) gradient descent by MLPs, which tend to overlook them in early to mid training.

1k Epochs (Full-Training Benchmarks)

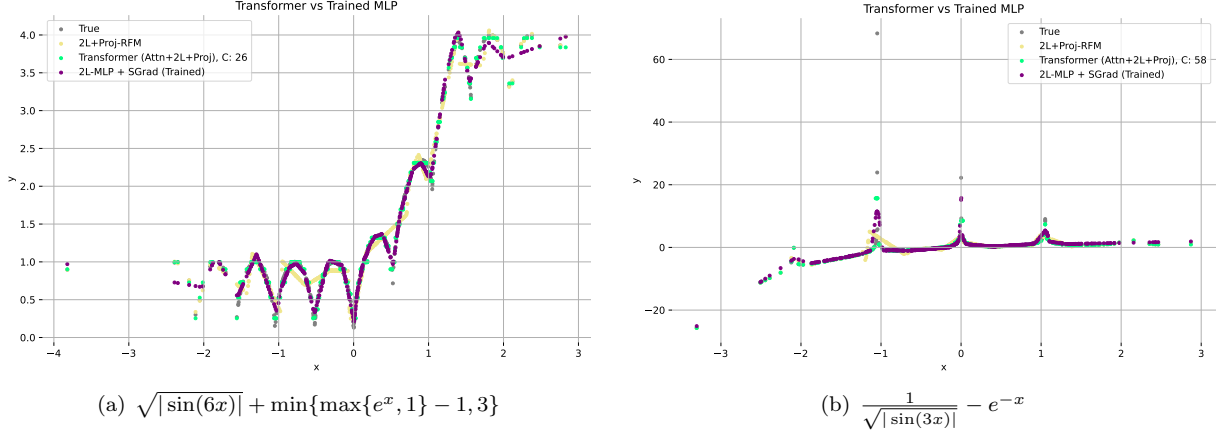


Figure 10: Comparison: A typical (100 epochs) trained (ADAM) 2-layer MLP vs. B) randomly initialized transformer with one attention head and 2 activated MLP layers and one trained final MLP output layer.

Conclusion: Even at initialization, one attention head can almost match the attention to detail possible with full MLP training by (stochastic) gradient descent.

7 Conclusion

Our result brings a comprehensive theory of deep learning within realistic sight by unifying the key statistical, approximation, and optimization components, rather than studying each of these pieces of the deep learning picture in mutual isolation. We do not rely on linearizing architectural simplifications, such as random feature models [80]/random neural networks [48] or neural tangent kernels [58], for analytic simplicity, which reduce the neural network to a kernel regressor; the latter of which has provably worse approximation rates⁹ [116].

Future Work The symmetric functions class, introduced in Definition 3.1, seem very natural in that they’re purely combinatorial structure means that they can be readily formulated on any compact metric space. This is in contrast to smoothness spaces which are classical vehicles for explaining favourable approximation [10, 103, 75, 1] and learning rates [107, Section 2.7] in deep learning, which heavily rely on a (locally) Euclidean structure of the underlying space to be defined (in any familiar sense). Therefore, unlike smoothness classes, we expect that our learning and approximation theory for symmetric function classes can be readily formulated within an infinite-dimensional operator learning [76, 63] or non-Euclidean geometric deep learning [66, 2] context with minor effort. However, we do not do so here to keep our material as transparent as possible.

8 Acknowledgements and Funding

A. Kratsios acknowledges financial support from an NSERC Discovery Grant No. RGPIN-2023-04482 and No. DGECR-2023-00230. They acknowledge that resources used in preparing this research were provided, in part, by the Province of Ontario, the Government of Canada through CIFAR, and companies sponsoring the Vector Institute¹⁰.

A Technicalities: General Setting and Explicit Assumptions

Setting A.1. Let $d, q, \kappa, N, F \in \mathbb{N}_+$, with $\kappa \leq q^d$, and let $\varepsilon > 0$. Fix a κ -symmetry \mathcal{S} at scale q . All target functions $f : \mathbb{R}^d \rightarrow \mathbb{R}^D$ will be assumed to be uniformly continuous with modulus of continuity ω .

Assumption A.1 (N, q , and F are Large Enough). In Setting A.1, we require:

$$(i) \ N \geq \left\lceil \frac{1}{4p^*} \sqrt{\log\left(\frac{Q^*}{\delta}\right) \left(\varepsilon^{-2} 64 \bar{\sigma}^2 \ln\left(\frac{Q^*}{2\delta}\right) + \log\left(\frac{Q^*}{\delta}\right)\right)} + 8\varepsilon^{-2} \bar{\sigma}^2 \ln\left(\frac{Q^*}{2\delta}\right) + \frac{\log\left(\frac{Q^*}{\delta}\right)}{4p^*} \right\rceil$$

⁹This is due to the gap between linear and non-linear widths [74].

¹⁰<https://vectorinstitute.ai/partnerships/current-partners/>

$$(ii) \quad q \geq \frac{\sqrt{d}}{\omega^{-1}(\sqrt{d}/\varepsilon)}$$

$$(iii) \quad F > \kappa^{5(1+\alpha)} \text{ and } F \geq \Delta_1^{C_1^2(1+\alpha)}$$

where the task complexity at scale q is $\Delta \stackrel{\text{def}}{=} \kappa^q$ (for absolute constants $C_1, \alpha > 0$ as in Theorem 5.1). Finally, we ask that $\mathbb{P}_X \in \mathcal{P}([0, 1]^d)$ is non-atomic.

B Proofs

B.1 Pre-Processing: Denoising Algorithm

Our ‘‘Purification’’ subroutine, which clearly runs in $\mathcal{O}(N^d)$ time, improves the quality of our training data while reducing its size. The next results show that given N large enough, the new input-output pair in any cube is approximately equal to the pair of the mid-point of that cube paired with *the true function value* at the midpoint. The remaining error decays to 0 as the cube side length goes to 0 (with a rate depending on the function’s regularity), and as the number of samples grows to ∞ , a precise convergence rate is given.

Lemma B.1 (Signal Recovery By Cube Averaging). *Let $d, D, q \in \mathbb{N}_+$, and $f : \mathbb{R}^d \rightarrow \mathbb{R}^D$ be continuous with modulus of continuity ω . Let Y_1, \dots, Y_N be such that: for each $n \in [N]$, $Y_n \stackrel{\text{def}}{=} f(X_n) + \varepsilon_n$ where $X_1, \dots, X_N \sim \mathbb{P}_X$ are random variables taking values in $[0, 1]^d$, and $\varepsilon_1, \dots, \varepsilon_N$ are independent centred (C, σ^2) -Sub-Gaussian¹¹ random variables. For each $Q \in \mathcal{Q}$, if there is an $X_n \in Q$ then: for each $t > 0$*

$$\left\| f(\bar{Q}) - \frac{1}{N_Q} \sum_{n=1}^{N_Q} Y_n \right\| \leq \omega\left(\frac{\sqrt{d}}{q}\right) + t \quad (25)$$

holds with probability at least $1 - 2e^{-N_Q t^2 / (8 \max\{1, \sigma\}^2)}$.

Proof of Lemma B.1. Let $N_Q \stackrel{\text{def}}{=} \#(\{X_n\}_{n=1}^N \cap Q)$ and note that $1 \leq N_Q \leq N$ by hypothesis. Without loss of generality, we reorder X_1, \dots, X_N such that $X_1, \dots, X_{N_Q} \in Q$. We thus compute

$$\begin{aligned} \left\| f(\bar{Q}) - \frac{1}{N_Q} \sum_{n=1}^{N_Q} Y_n \right\| &\leq \left\| \frac{1}{N_Q} \sum_{n=1}^{N_Q} f(\bar{Q}) - \frac{1}{N_Q} \sum_{n=1}^{N_Q} Y_n \right\| \\ &\leq \left\| \frac{1}{N_Q} \sum_{n=1}^{N_Q} f(\bar{Q}) - \frac{1}{N_Q} \sum_{n=1}^{N_Q} f(X_n) + \varepsilon_n \right\| \\ &\leq \left\| \frac{1}{N_Q} \sum_{n=1}^{N_Q} (f(\bar{Q}) - f(X_n)) - 0 - \frac{1}{N_Q} \sum_{n=1}^{N_Q} \varepsilon_n \right\| \\ &\leq \left\| \frac{1}{N_Q} \sum_{n=1}^{N_Q} (f(\bar{Q}) - f(X_n)) \right\| + \left\| 0 - \frac{1}{N_Q} \sum_{n=1}^{N_Q} \varepsilon_n \right\| \\ &\leq \frac{1}{N_Q} \sum_{n=1}^{N_Q} \|f(\bar{Q}) - f(X_n)\| + \left\| 0 - \frac{1}{N_Q} \sum_{n=1}^{N_Q} \varepsilon_n \right\| \\ &\leq \omega(\|\bar{Q} - X_n\|) + \left\| 0 - \frac{1}{N_Q} \sum_{n=1}^{N_Q} \varepsilon_n \right\| \\ &\leq \omega\left(\frac{\sqrt{d}}{q}\right) + \left\| 0 - \frac{1}{N_Q} \sum_{n=1}^{N_Q} \varepsilon_n \right\| \end{aligned} \quad (26)$$

$$\leq \omega\left(\frac{\sqrt{d}}{q}\right) + \left\| 0 - \frac{1}{N_Q} \sum_{n=1}^{N_Q} \varepsilon_n \right\| \quad (27)$$

¹¹I.e. $\mathbb{P}(\|\varepsilon_1\| > t) \leq Ce^{-t^2/2\sigma^2}$ for all $t > 0$.

where (26) holds since $\text{diam}(Q) = \sqrt{d}/q$. Since the empirical mean of N_Q (C, σ^2) sub-Gaussian random variables is $(2, \frac{4}{N_Q} \sum_{n=1}^{N_Q} \sigma^2)$ sub-Gaussian, see e.g. [56, Lemma 22] then: for each $t > 0$ we have

$$\mathbb{P}\left(\left\|\frac{1}{N_Q} \sum_{n=1}^{N_Q} X_n\right\| < t\right) \geq 1 - 2e^{-t^2/(8\tilde{\sigma}^2)} \quad (28)$$

where $\tilde{\sigma}^2 \stackrel{\text{def.}}{=} \frac{1}{N_Q^2} \sum_{n=1}^{N_Q} \max\{1, \sigma\}^2 = \frac{1}{N_Q^2} \max\{1, \sigma\}$. Thus, together (27) and (28) imply that: for every $t > 0$ equation (25) holds with probability at least $1 - 2e^{-N_Q t^2/(8 \max\{1, \sigma\}^2)}$. \square

Lemma B.2 (Success Rate of Algorithm 1). *In the setting of Lemma B.1, fix a failure rate probability $0 < \delta \leq 1$, a quantization size q , and a samples size N ; where $N, q \in \mathbb{N}_+$. Let $\bar{\mathcal{D}}$ be the output of Algorithm 1. Let $\mathcal{Q}^* \stackrel{\text{def.}}{=} \#(\text{supp}(\mathbb{P}_X) \cap \mathcal{Q}) \in [q^d]$ represent the “intrinsic dimension at scale q ” and let $\bar{\sigma} \stackrel{\text{def.}}{=} \max\{1, \sigma\}$. If N is “large enough”; meaning that*

$$N \geq \left\lceil \frac{1}{4p^*} \sqrt{\log\left(\frac{\mathcal{Q}^*}{\delta}\right) \left(\frac{64\bar{\sigma}^2 \ln\left(\frac{\mathcal{Q}^*}{2\delta}\right)}{\omega(\sqrt{d}/q)^2} + \log\left(\frac{\mathcal{Q}^*}{\delta}\right)\right)} + \frac{8\bar{\sigma}^2 \ln\left(\frac{\mathcal{Q}^*}{2\delta}\right)}{\omega(\sqrt{d}/q)^2} + \frac{\log\left(\frac{\mathcal{Q}^*}{\delta}\right)}{4p^*} \right\rceil. \quad (29)$$

then: for all $Q \in \mathcal{Q}$, both $N_Q \stackrel{\text{def.}}{=} \#\{\{X_n\}_{n=1}^N \in Q\} > 0$ and

$$\max_{Q \in \mathcal{Q}} \left\| f(\bar{Q}) - \frac{1}{N_Q} \sum_{(X,Y) \in Q} Y_Q \right\| \leq 2\omega(\sqrt{d}/q) \quad (30)$$

hold with probability at-least $1 - \delta > 0$ (on the draw of $\{(X_n, Y_n)\}_{n=1}^N$).

Proof of Lemma B.2. Fix a minimum sample size per cube $M \in \mathbb{N}_+$, with $Mq^d \leq N$. We now argue in 3 steps.

Step 0 - Derandomization Lower Bound:

For each $Q \in \mathcal{Q}_{i,s}$ we denote $N_Q \stackrel{\text{def.}}{=} \#\{\{X_n\}_{n=1}^N \in Q\}$. Fix $M \in \mathbb{N}_+$ with $M \leq N_Q$. We first begin with the following “de-ranomization” lower bound

$$\begin{aligned} \text{(I)} &\stackrel{\text{def.}}{=} \mathbb{P}\left(\max_{Q \in \mathcal{Q}_{i,s}} \left| f(\bar{Q}) - \frac{1}{N_Q} \sum_{(X,Y) \in Q} Y_Q \right| \leq \omega(\sqrt{d}/q) + t\right) \\ &= \sum_{m=1}^N \mathbb{P}\left(\max_{Q \in \mathcal{Q}_{i,s}} \left| f(\bar{Q}) - \frac{1}{N_Q} \sum_{(X,Y) \in Q} Y_Q \right| \leq \omega(\sqrt{d}/q) + t \mid \min_{Q \in \mathcal{Q}_{i,s}} N_Q = m\right) \\ &\quad \times \mathbb{P}\left(\min_{Q \in \mathcal{Q}_{i,s}} N_Q = m\right) \\ &\geq \underbrace{\mathbb{P}\left(\max_{Q \in \mathcal{Q}} \left| f(\bar{Q}) - \frac{1}{N_Q} \sum_{(X,Y) \in Q} Y_Q \right| \leq \omega(\sqrt{d}/q) + t \mid \min_{Q \in \mathcal{Q}} N_Q \geq M\right)}_{\text{(II)}} \\ &\quad \times \underbrace{\mathbb{P}(\forall Q \in \mathcal{Q} \ N_Q \geq M)}_{\text{(III)}} \end{aligned}$$

Step 1 - The Conditional Signal Recovery Probability (Term (II)):

Applying Lemma B.1, conditional on $N_Q \geq M$ for each $Q \in \mathcal{Q}$, and taking a union bound indexed by $Q \in \mathcal{Q}$, we have: for every $t > 0$

$$\begin{aligned} \text{(II)} &= \mathbb{P}\left(\max_{Q \in \mathcal{Q}} \left| f(\bar{Q}) - \frac{1}{N_Q} \sum_{(X,Y) \in Q} Y_Q \right| \leq \omega(\sqrt{d}/q) + t \mid \min_{Q \in \mathcal{Q}} N_Q \geq M\right) \\ &\geq 1 - \sum_{Q \in \mathcal{Q}} \mathbb{P}\left(\left\| f(\bar{Q}) - \frac{1}{N_Q} \sum_{(X,Y) \in Q} Y_Q \right\| \leq \omega(\sqrt{d}/q) + t \mid \min_{Q \in \mathcal{Q}} N_Q \geq M\right) \\ &\geq 1 - 2\mathcal{Q}^* e^{-Mt^2/(8\bar{\sigma}^2)} \quad (31) \end{aligned}$$

where $\bar{\sigma} \stackrel{\text{def.}}{=} \max\{1, \sigma\} > 0$ and $\mathcal{Q}^* \stackrel{\text{def.}}{=} \#(\text{supp}(\mathbb{P}_X) \cap \mathcal{Q})$. Let $0 < \delta_R \leq 1$ be the conditional recovery failure probability, then setting $\delta_R \geq 2q^d e^{-M t^2 / (8\bar{\sigma}^2)}$ and solving for M implies that the right-hand side of (31) is bounded below by $1 - \delta_R$ if

$$\frac{8\bar{\sigma}^2 \ln(\mathcal{Q}^* / (2\delta_R))}{t^2} \leq M. \quad (32)$$

It remains to bound the probability in (III) below.

Step 2 - The Probability of Observing M Samples/Cube (Term (III)):

The control of (III) is equivalent to a coupon collection problem¹² with non-uniform weights. To this end, for each $Q \in \mathcal{Q}_{i,s}$ consider the counting process $N_\tau^{(Q)}$ defined for each $\tau \in \mathbb{N}_+$ by $N_\tau^{(Q)} \stackrel{\text{def.}}{=} \sum_{u=1}^\tau I_{X_u \in Q}$. For each $\tau \in \mathbb{N}_+$, upon taking a union bound we have

$$\mathbb{P}\left(\min_{Q \in \mathcal{Q}_{i,s}} N_\tau^{(Q)} < M\right) \leq \sum_{Q \in \mathcal{Q}_{i,s}} \mathbb{P}\left(N_\tau^{(Q)} < M\right). \quad (33)$$

Since the $(I_{X_s \in Q})_{u=1}^t$ are i.i.d. a Bernoulli trials and thus they have success probability at-least $p_* > 0$ then by [51, Theorem 1], we have: for each $Q \in \mathcal{Q}_{i,s}$ and $\tau \in \mathbb{N}_+$, if $0 < M/\tau \leq p_* \leq 1$ then

$$\mathbb{P}\left(N_\tau^{(Q)} < M\right) \leq e^{-\text{KL}(\text{Ber}(M/\tau) \parallel \text{Ber}(p_*))} \stackrel{\text{def.}}{=} e^{-\left(\frac{M}{\tau} \ln\left(\frac{M}{\tau p_*}\right) + \left(1 - \frac{M}{\tau}\right) \ln\left(\frac{1 - M/\tau}{1 - p_*}\right)\right)} \quad (34)$$

where $\text{Ber}(p) \stackrel{\text{def.}}{=} p\delta_1 + (1-p)\delta_0$. Incorporating (34) into the right-hand side of (33) yields

$$\mathbb{P}\left(\min_{Q \in \mathcal{Q}_{i,s}} N_\tau^{(Q)} < M\right) \leq \mathcal{Q}^* e^{-\left(\frac{M}{\tau} \ln\left(\frac{M}{\tau p_*}\right) + \left(1 - \frac{M}{\tau}\right) \ln\left(\frac{1 - M/\tau}{1 - p_*}\right)\right)} \quad (35)$$

where we have used the fact that $\mathcal{Q}^* = \#\mathcal{Q}_{i,s}$. By [51, Equations (2.2)-(2.3)], we have the inequality

$$\begin{aligned} 2(p_* - M/\tau)^2 &\leq \text{KL}(\text{Ber}(M/\tau) \parallel \text{Ber}(p_*)) \\ &= \left(\frac{M}{\tau} \ln\left(\frac{M}{\tau p_*}\right) + \left(1 - \frac{M}{\tau}\right) \ln\left(\frac{1 - M/\tau}{1 - p_*}\right)\right). \end{aligned} \quad (36)$$

Now, (36) implies that the right-hand side of (35) further simplifies to

$$\mathbb{P}\left(\min_{Q \in \mathcal{Q}_{i,s}} N_\tau^{(Q)} < M\right) \leq \mathcal{Q}^* e^{-2\tau(q_* - M/\tau)^2}. \quad (37)$$

Thus, for every number of coupons collected $t \in \mathbb{N}_+$ (samples drawn) we have

$$\mathbb{P}\left(\min_{Q \in \mathcal{Q}_{i,s}} N_\tau^{(Q)} \geq M\right) \leq 1 - \mathcal{Q}^* e^{-\tau(q_* - M/\tau)^2/2}. \quad (38)$$

Fix $N = \tau > 1$. Let $0 < \delta_S \leq 1$ be the ‘‘sampling failure probability’’ then, setting $\mathcal{Q}^* e^{-(q_* - M/\tau)^2/2} \leq \delta_S$, temporarily letting $\tau > 0$ be real, and solving for τ yields

$$\tau \geq \frac{\sqrt{\log(\mathcal{Q}^*/\delta_S)(8M + \log(\mathcal{Q}^*/\delta_S))} + 4Mp_* + \log(\mathcal{Q}^*/\delta_S)}{4p_*} \quad (39)$$

provided that $\log\left(\frac{\mathcal{Q}^*}{\delta}\right) > 0$; i.e. $0 < \delta < \mathcal{Q}^*$ (but this always holds since $\mathcal{Q}^* \geq 1$ and $\delta \leq 1$). Taking integer ceilings across (39) implies that: if

$$N \geq \left\lceil \frac{\sqrt{\log(\mathcal{Q}^*/\delta_S)(8M + \log(\mathcal{Q}^*/\delta_S))} + 4Mp_* + \log(\mathcal{Q}^*/\delta_S)}{4p_*} \right\rceil \quad (40)$$

then

$$(III) = \mathbb{P}(\forall Q \in \mathcal{Q}_{i,s}^* N_Q \geq M) \geq 1 - \delta_S > 0. \quad (41)$$

As both terms (II) and (III) have been bounded below then we obtain the conclusion upon setting $\delta = \delta_S = \delta_R$; yields the conclusion.

¹²More precisely, this is a Double-Dixie cub variant of the coupon collector’s problem.

Step 3 - Counting The Required Number of Samples:

Reconciling expressions (32) with (40), we have

$$N \geq \left\lceil \frac{\sqrt{\log\left(\frac{Q^*}{\delta_S}\right) \left(8 \frac{8\bar{\sigma}^2 \ln\left(\frac{Q^*}{2\delta_R}\right)}{t^2} + \log\left(\frac{Q^*}{\delta_S}\right)\right) + 4 \frac{8\bar{\sigma}^2 \ln\left(\frac{Q^*}{2\delta_R}\right)}{t^2} p^* + \log\left(\frac{Q^*}{\delta_S}\right)}{4p^*} \right\rceil. \quad (42)$$

Consequently, the following lower bound holds

$$(I) \geq (II) \times (III) \geq (1 - \delta_R)(1 - \delta_S).$$

For simplicity, we retroactively couple $t \stackrel{\text{def.}}{=} \omega\left(\frac{\sqrt{d}}{q}\right)$, then (42) simplifies to

$$N \geq \left\lceil \frac{\sqrt{\log\left(\frac{Q^*}{\delta_S}\right) \left(8 \frac{8\bar{\sigma}^2 \ln\left(\frac{Q^*}{2\delta_R}\right)}{\omega(\sqrt{d}/q)^2} + \log\left(\frac{Q^*}{\delta_S}\right)\right) + 4 \frac{8\bar{\sigma}^2 \ln\left(\frac{Q^*}{2\delta_R}\right)}{\omega(\sqrt{d}/q)^2} p^* + \log\left(\frac{Q^*}{\delta_S}\right)}{4p^*} \right\rceil. \quad (43)$$

Now fix an overarching failure probability $0 < \delta \leq 1$, retroactively couple $\delta_R = \delta_S$ and $(1 - \delta_R)(1 - \delta_S) = 1 - \delta$. Then,

$$\delta_R = \delta_S = 1 - \sqrt{1 - \delta} \quad (44)$$

and note that, for each $0 < \delta \leq 1$ we indeed have $1 - \sqrt{1 - \delta} \in (0, 1]$; whence both $\delta_R, \delta_S \in (0, 1]$ are indeed well-defined failure probabilities. Incorporating our retroactive couplings in (44) into (43) yields the lower bound on N in (29). \square

Proposition B.1 (Success Rate of Algorithm 1). *In the setting of Lemma B.1 suppose that ω is strictly increasing and continuous. Fix an recovery error $\varepsilon > 0$ and a failure probability $0 < \delta \leq 1$. If the scale $q \in \mathbb{N}_+$ satisfies*

$$q \geq \frac{\sqrt{d}}{\omega^{-1}(\sqrt{d}/\varepsilon)} \quad (45)$$

then, if the sample size N is at least

$$N \geq \left\lceil \frac{1}{4p^*} \sqrt{\log\left(\frac{Q^*}{\delta}\right) \left(\varepsilon^{-2} 64 \bar{\sigma}^2 \ln\left(\frac{Q^*}{2\delta}\right) + \log\left(\frac{Q^*}{\delta}\right)\right) + 8\varepsilon^{-2} \bar{\sigma}^2 \ln\left(\frac{Q^*}{2\delta}\right) + \frac{\log\left(\frac{Q^*}{\delta}\right)}{4p^*}} \right\rceil. \quad (46)$$

then: for all $Q \in \mathcal{Q}_{\mathbb{P}} \stackrel{\text{def.}}{=} \mathcal{Q} \cap \text{supp}(\mathbb{P}_X)$, both $N_Q \stackrel{\text{def.}}{=} \#\{\{X_n\}_{n=1}^N \in Q\} > 0$ and

$$\mathbb{P}\left(\max_{Q \in \mathcal{Q}_{\mathbb{P}}} \left\| f(\bar{Q}) - \frac{1}{N_Q} \sum_{(X,Y) \in Q} Y_Q \right\| \leq \varepsilon \right) \geq 1 - \delta.$$

Proof of Proposition B.1. Since ω is continuous and strictly increasing, then ω^{-1} is well-defined. The result now follows from Lemma B.2 with q satisfying (45). \square

We are now in place to prove Proposition 4.1, which is the less technical version of Proposition B.1 above.

Proof of Proposition 4.1. By [2, Lemma 7.1], since the ℓ^∞ -doubling dimension of $\text{supp}(\mathbb{P})$ is \bar{d} then the $1/q$ -covering number of $\text{supp}(\mathbb{P}_X)$ with respect to the ℓ^∞ metric, namely, Q^* satisfies

$$Q^* \leq (2^{\bar{d}})^{\lceil \log_2(q) \rceil} \leq 2q^{\bar{d}} \leq 2\varepsilon^{-\bar{d}} L^{\bar{d}}.$$

The result now follows from Proposition 4.1 if

$$N \geq \left\lceil \frac{c\bar{\sigma}^2 \varepsilon^{-2}}{p^*} \left(\log^2 \left(\frac{2\varepsilon^{-\bar{d}} L^{\bar{d}}}{\delta} \right) \right) \right\rceil \in \Omega(\varepsilon^{-2} \log^2(1/(\varepsilon\delta))) \quad (47)$$

where $c = 64$. \square

B.2 Pre-Training (Domain Adaptation)

This appendix contains the proof of the main results in sub-section 4.2. The clustering portion of Algorithm 2 is based on the following lemma which states that, whenever the conclusion of Lemma B.2 holds then, clustering on the output values of Algorithm 1 with a very small threshold implies clustering on the true function itself.

Lemma B.3 (Clustering on Data with Small Threshold Implies Clustering on Function Values). *In the setting of Lemma B.2, fix a failure probability $0 < \delta \leq 1$ and let N satisfy (29). Fix $\varepsilon > 0$ and suppose that the scale q satisfies*

$$\frac{\sqrt{d}}{\omega^\dagger(\varepsilon/2^5)} \leq q \quad (48)$$

and suppose that $f(\{\bar{Q}\}_{Q \in \mathcal{Q}^})$ is ε -separated. The following holds with probability at-least $1 - \delta$ on the draw of $\{(X_n, Y_n)\}_{n=1}^N$:*

For every $Q_1, Q_2 \in \mathcal{Q}^$ the following are equivalent*

$$\|Y_{Q_1} - Y_{Q_2}\|_2 \leq \frac{\varepsilon}{2^3} \Leftrightarrow \|f(\bar{Q}_1) - f(\bar{Q}_2)\|_2 \leq \varepsilon \quad (49)$$

where for every $Q \in \mathcal{Q}^$ we write $Y_Q \stackrel{\text{def.}}{=} \frac{1}{N_Q} \sum_{X_n \in Q} Y_n$.*

Proof of Lemma B.3. With probability $1 - \delta$, on the draw of $\{(X_n, Y_n)\}_{n=1}^N$, the conclusion of Lemma B.2 holds. Conditioned on (30) holding, we have that: for every $Q \in \mathcal{Q}^*$ $Q \cap \{X_n\}_{n=1}^N \neq \emptyset$ thus, each $Y_Q \stackrel{\text{def.}}{=} \frac{1}{N_Q} \sum_{X_n \in Q} Y_n$ is well-defined. Now, still conditioned on (30) holding, for each $Q_1, Q_2 \in \mathcal{Q}^*$

$$\|f(\bar{Q}_1) - f(\bar{Q}_2)\|_2 \leq \|Y_{Q_1} - Y_{Q_2}\|_2 + \sum_{i=1}^2 \|f(\bar{Q}_i) - Y_{Q_i}\|_2 \quad (50)$$

$$\begin{aligned} &\leq \|Y_{Q_1} - Y_{Q_2}\|_2 + 4\omega(\sqrt{d}/2) \\ &\leq \|Y_{Q_1} - Y_{Q_2}\|_2 + \varepsilon/8 \end{aligned} \quad (51)$$

where (51) held by since q satisfied (48). Therefore, still conditioned on (30) holding, for each $Q_1, Q_2 \in \mathcal{Q}^*$ (50) implies that

$$\|f(\bar{Q}_1) - f(\bar{Q}_2)\|_2 - \varepsilon/8 \leq \|Y_{Q_1} - Y_{Q_2}\|_2. \quad (52)$$

Consequently, if $\|f(\bar{Q}_1) - f(\bar{Q}_2)\|_2 > \varepsilon$ then (52) implies that

$$\|Y_{Q_1} - Y_{Q_2}\|_2 > \frac{7}{8}\varepsilon > \varepsilon/8.$$

This proves the first direction of (49).

We show the other direction by contraposition. Still conditioned on (30) holding, Suppose that: $Q_1, Q_2 \in \mathcal{Q}^*$ are such that

$$\|f(\bar{Q}_1) - f(\bar{Q}_2)\|_2 < \varepsilon. \quad (53)$$

The ε -separatedness of $f(\{Q\}_{Q \in \mathcal{Q}^*})$ implies that

$$\min_{y, \tilde{y} \in f(\{Q\}_{Q \in \mathcal{Q}^*}); y \neq \tilde{y}} \|y - \tilde{y}\| \geq \varepsilon. \quad (54)$$

Together (53) and (54) imply that

$$\|f(\bar{Q}_1) - f(\bar{Q}_2)\|_2 = 0. \quad (55)$$

Since $f(\{Q\}_{Q \in \mathcal{Q}^*})$ is ε -separated Then, again by Lemma B.2, (30) implies that

$$\|Y_{Q_1} - Y_{Q_2}\|_2 \leq \|f(\bar{Q}_1) - f(\bar{Q}_2)\|_2 + \sum_{i=1}^2 \|f(\bar{Q}_i) - Y_{Q_i}\|_2 \quad (56)$$

$$\begin{aligned} &\leq \|f(\bar{Q}_1) - f(\bar{Q}_2)\|_2 + 4\omega(\sqrt{d}/2) \\ &\leq \varepsilon/8 \end{aligned} \quad (57)$$

where (57) held by (55). Thus, (53) implies that $\|Y_{Q_1} - Y_{Q_2}\|_2 \leq \varepsilon/8$ and by constraposition

$$\|Y_{Q_1} - Y_{Q_2}\|_2 > \varepsilon/8 \Leftrightarrow \|f(\bar{Q}_1) - f(\bar{Q}_2)\|_2 \geq \varepsilon.$$

This completes our proof. \square

This lemma justifies the following algorithm to be run following Algorithm 1.

Lemma B.4 (Cluster Identification Property of Max-Temperature Attention Initialized by Algorithm 2). *In the setting of Lemma B.3, let $\mathcal{C}, \mathcal{D}, V$ and K be as in Algorithm 2 with input $\mathcal{D} = \mathcal{D}^* = \{(x_c, y_c)\}_{c \in \mathcal{C}}$ from Algorithm 1. Then, $d_c \stackrel{\text{def.}}{=} \#\mathcal{C} = C$, $d_k = \#\mathcal{D}^* \leq q^d$, and the map $\text{Attn}(\cdot|K, V) : \mathbb{R}^d \rightarrow \mathbb{R}^d$ satisfies the cluster identifiability property*

$$\text{Attn}(x|K, V) = \frac{1}{\sqrt{d}}x_c \Leftrightarrow (\forall Q \in \mathcal{C}) f(\bar{Q}) = y_c$$

for all $x \in \mathcal{G} \stackrel{\text{def.}}{=} \mathbb{R}^d \setminus \bigcup_{c \in \mathcal{C}, Q \in \mathcal{C}} \partial Q$.

Proof of Lemma B.4. Consider the “bad set” $\mathcal{B} \stackrel{\text{def.}}{=} \bigcup_{c \in \mathcal{C}, Q \in \mathcal{C}} \partial Q$ and the “good set” $\mathcal{G} \stackrel{\text{def.}}{=} \mathbb{R}^d \setminus \mathcal{B}$. Define the Voronoi cells $\{\tilde{V}_c\}_{c \in \mathcal{C}}$ for each $c \in \mathcal{C}$ by

$$\tilde{V}_c \stackrel{\text{def.}}{=} \{x \in \mathbb{R}^d : \|x - \tilde{V}_c\| = \min_{\tilde{c} \in \mathcal{C}} \|x - \tilde{V}_{\tilde{c}}\|\}.$$

We now, modify the Voronoi cells into a partition $\{V_c\}_{c \in \mathcal{C}}$ by

$$V_c \stackrel{\text{def.}}{=} \tilde{V}_c \setminus \bigcup_{\tilde{c} \in \mathcal{C}; \tilde{c} \neq c} \tilde{V}_{\tilde{c}}.$$

Notice that, for any distinct $c, \tilde{c} \in \mathcal{C}$ since $\tilde{V}_c \cap \tilde{V}_{\tilde{c}} \subseteq \mathcal{B}$; thus,

$$V_c \cap \mathcal{G} = \tilde{V}_c \cap \mathcal{G} \text{ for all } c \in \mathcal{C}. \quad (58)$$

Therefore, the map $\text{proj} : \mathbb{R}^d \rightarrow [C]$ defined for each $x \in \mathbb{R}^d$ by

$$\text{proj}(x) \stackrel{\text{def.}}{=} \sum_{c=1}^C e_c I_{x \in V_c}$$

where $\{e_c\}_{c=1}^C$ is the standard (ordered) orthonormal basis of \mathbb{R}^C . Since, for every $c \in \mathcal{C}$, $V_c \subseteq \tilde{V}_c$, then by definition of the Voronoi cells,

$$\text{proj}(x) \in \bigcup_{Q \in \mathcal{C}} Q \Leftrightarrow c \in \underset{c \in \mathcal{C}}{\text{argmin}} \|x - \bigcup_{Q \in \mathcal{C}} Q\|_\infty \quad (59)$$

where, recall that, for any non-empty $A \subseteq \mathbb{R}^d$ and any $x \in \mathbb{R}^d$ we set $\|x - A\|_\infty \stackrel{\text{def.}}{=} \inf_{z \in A} \|x - z\|_\infty$. Now, since $\{\mathcal{G} \cap \bigcup_{Q \in \mathcal{C}} Q\}_{c \in \mathcal{C}}$ are disjoint then for each $x \in \mathcal{G}$ there exists a unique $c \in \mathcal{C}$ such that $x \in \mathcal{G} \cap \bigcup_{Q \in \mathcal{C}} Q$; therefore, there exists a unique $Q \in \mathcal{Q}$ such that

$$\|x - Q\|_\infty = \min_{\tilde{Q} \in \mathcal{Q}} \|x - \tilde{Q}\|_\infty.$$

Therefore, for each $x \in \mathcal{G}$, $\#\text{argmax}_{Q \in \mathcal{Q}} \|x - Q\|_\infty = 1$ and consequently there exists a unique $n \in [q^d]$ such that $\#\text{argmax}_{Q \in \mathcal{Q}} \|x - Q\|_\infty = 1$. Therefore, for each $i \in [q^d]$ and every $x \in \mathcal{G}$ we have

$$\begin{aligned} \text{Softmax}_\infty \left(-\bigoplus_{n=1}^{q^d} \|x - x_n\|_\infty \right)_i &= \frac{I_{\|x - x_i\|_\infty = \max_{u \in [q^d]} \|x - x_u\|_\infty}}{\#\text{argmax}_{v \in [q^d]} \|x - x_v\|_\infty} \\ &= I_{\|x - x_i\|_\infty = \max_{u \in [q^d]} \|x - x_u\|_\infty}. \end{aligned}$$

Therefore, for each $x \in \mathcal{G}$, $\text{Softmax}_\infty \left(-\bigoplus_{n=1}^{q^d} \|x - x_n\|_\infty \right) = \text{proj}(x)$. Therefore, the map $\text{Attn}(x|K, V)$ satisfies the ℓ^∞ -metric projection property:

$$\begin{aligned} \text{Attn}(x|K, V) &= \left(\frac{1}{\sqrt{d}}x \right)_{x \in \mathcal{D}^*}^\top \text{proj}(x) \\ \text{s.t. } \text{proj}(x) &\in \underset{c \in \mathcal{C}}{\text{argmin}} \|x - \bigcup_{Q \in \mathcal{C}} Q\|_\infty \end{aligned} \quad (60)$$

for all $x \in \mathcal{G}$. Now, applying Lemma B.2, we know that with probability at-least $1 - \delta$ (on the draw of $\{(X_n, Y_n)\}_{n=1}^N$) (49) holds. Thus, the definition of the disjoint Voronoi cells $\{V_c\}_{c \in \mathcal{C}}$ we have that: for each $x \in \mathcal{G}$

$$\text{Attn}(x|K, V) = \frac{1}{\sqrt{d}}x_c \Leftrightarrow \forall Q \in \mathcal{C} f(\bar{Q}) = y_c,$$

again, while conditioned on the draw of $\{(X_n, Y_n)\}_{n=1}^N$. This concludes our proof. \square

Lemma B.5 (Algorithm Generates Separated and Norm-Bounded Input Features). *Fix a failure probability $0 < \delta \leq 1$ and let N satisfy (29) and suppose that F satisfies (14). Then, the following holds with probability at-least $1 - \delta$ (on the draw of $\{(X_n, Y_n)\}_{n=1}^N$): in the setting of Lemma B.4, we have*

$$\underbrace{\max_{x \in \mathcal{D}^*} \left\| \frac{1}{\sqrt{d}} x \right\|_2}_{\text{Norm-Boundedness}} \quad \text{and} \quad \underbrace{C \sqrt{\frac{(1+\alpha) \log \#\mathcal{C}}{\log F}}}_{\text{Sufficient separation}} \leq \min_{\substack{x, \tilde{x} \in \mathcal{D}^* \\ x \neq \tilde{x}}} \left\| \frac{1}{\sqrt{d}} x - \frac{1}{\sqrt{d}} \tilde{x} \right\|_2$$

for the constant $C > 0$ in Proposition B.3.

i.e. satisfies the conditions of Proposition B.3.

Proof of Lemma B.5. Step 1 - Verifying Separation

By construction $\{x_n\}_{n=1}^{q^d}$ is an $1/q$ packing of $[0, 1]^d$ in the ℓ^∞ -norm. Whence, for each distinct $n, m \in [q^d]$ we have

$$\frac{1}{q} \leq \|x_n - x_m\|_\infty \leq \|x_n - x_m\|_2 \quad (61)$$

where we used the fact that $\|\cdot\|_\infty \leq \|\cdot\|_2$ on \mathbb{R}^d . Rescaling (61) by a factor of $\frac{1}{\sqrt{d}}$ (as in the definition of the values matrix in V in Algorithm 2) implies that

$$\frac{1}{\sqrt{d}q} \leq \min_{x, \tilde{x} \in \mathcal{D}^*; x \neq \tilde{x}} \left\| \frac{1}{\sqrt{d}} x - \frac{1}{\sqrt{d}} \tilde{x} \right\|_2. \quad (62)$$

Therefore, (62) implies that the separation condition in Proposition B.3 for the input data \mathcal{D}^* , where \mathcal{D}^* is as in Algorithm 2, holds if

$$C \sqrt{\frac{(1+\alpha) \log \#\mathcal{C}}{\log F}} \leq \frac{1}{q} \quad (63)$$

since $\#\mathcal{D}^* = \#\mathcal{C}$. Isolating q in (63) yields the desired inequality in (14).

Step 2 - Verifying Separation

We now verify that condition $\|x\|_2 \leq 2$ for each datum $x \in \mathcal{D}^*$ to verify all the conditions of Proposition B.3; for this, simply note that

$$\max_{x \in \mathcal{D}^*} \left\| \frac{1}{\sqrt{d}} x \right\|_2 \leq \frac{1}{\sqrt{d}} \sup_{x \in [0, 1]^d} \|x\|_2 = \frac{1}{\sqrt{d}} \sqrt{\sum_{i=1}^d 1^2} = 1.$$

Whence, the conclusion of Proposition B.3 are met by the data \mathcal{D}^* . \square

Putting the above lemmata together yields the main result of this section.

Proof of Proposition 4.2. Directly follows from Lemmata B.4 and B.5 conditioned on the draw of $\{(X_n, Y_n)\}_{n=1}^N$. \square

B.2.1 Well-Conditioned (Random) Deep Feature Matrix

Proposition B.2 (Shallow ReLU Random Features). *Fix sufficiently large integers $F, N \in \mathbb{N}$ such that $F > N^{5(1+\alpha)}$ for some absolute constant $\alpha > 0$. Let $X \in \mathbb{R}^{d \times N}$ with columns $\{x_1, \dots, x_N\} \subset \mathbb{R}^d$ such that*

$$\|x_i\|_2 \in [0, 2], \quad \forall i = 1, \dots, N, \quad \|x_i - x_j\|_2 \geq C \sqrt{\frac{(1+\alpha) \log N}{\log F}}, \quad \forall i \neq j$$

for some absolute constant $C > 0$. Let $B \in \mathbb{R}^{F \times d}$ be a random standard Gaussian matrix. There exists a $b \in \mathbb{R}$ solving the implicit equation

$$p \stackrel{\text{def.}}{=} \frac{C \log^2(2NF)}{N^{-2(1+\alpha)} F} > 0 \quad \text{and} \quad p = b^2 (1 - \Phi_{CDF}(b)) - \frac{b}{\sqrt{2\pi}} e^{-\frac{b^2}{2}}$$

where Φ_{CDF} is the standard Gaussian CD. Then with probability at least $1 - N^{-3-20(1+\alpha)}$ over the draw of B , the random feature matrix

$$\Psi = \frac{1}{\sqrt{Fp}} \text{ReLU}(BX + b\mathbf{1}_F \mathbf{1}_N^\top) \in \mathbb{R}^{F \times N}$$

is well-conditioned:

$$\max_{i=1, \dots, N} |s_i(\Psi) - 1| \leq N^{-\alpha/2}.$$

Proof. Define $b > 0$ by

$$p = \mathbb{E}_{\gamma \sim N(0,1)}(\text{ReLU}(\gamma - b)^2). \quad (64)$$

Set $\varepsilon = N^{-(1+\alpha)}$ where N is number of inputs and $\alpha > 0$ arbitrary fixed constant. Then every pair x_i, x_j of inputs satisfy the separation requirement in Lemma C.1 for some large absolute constant C . Also, the size of F, N, p, b all satisfies the requirement in Lemma C.1. Then with probability at least $1 - 4F(2NF)^{-5}$, we have

$$|\|\psi_i\|_2^2 - 1| \leq \varepsilon, \quad |\langle \psi_i, \psi_j \rangle| \leq \epsilon$$

where ψ_i is the i -th column of Ψ . By union bound, with probability at least $1 - N^2 \cdot 4F(2NF)^{-5} > 1 - N^{-3-20(1+\alpha)}$, we have

$$|\|\psi_i\|_2^2 - 1| \leq \varepsilon, \quad |\langle \psi_i, \psi_j \rangle| \leq \epsilon$$

for all i, j . Since G is symmetric, then the spectral theorem implies that its eigenvalues are in \mathbb{R} . Consider the covariance $G = \Psi^\top \Psi \in \mathbb{R}^{N \times N}$. This, together with the Gershgorin Circle Theorem, see e.g. [53, Theorem 6.2.5], we can see that the eigenvalues of G is bounded between $[1 - N\epsilon, 1 + N\epsilon] = [1 - N^{-\alpha}, 1 + N^{-\alpha}]$. Taking the square root we obtain the singular values of Ψ .

It remains to analyze b . As shown on [14, page 90, just before section 2.1] if $Z \sim N(\mu, \sigma)$ for some $\mu \in \mathbb{R}$ and $\sigma > 0$, then $Z^+ \stackrel{\text{def.}}{=} \text{ReLU}(Z)$ has second non-central moment given by

$$\text{Var}(Z^+) = \left(\mu^2 + \sigma^2\right) \left(1 - \Phi_{CDF}\left(-\frac{\mu}{\sigma}\right)\right) + \frac{\mu\sigma}{\sqrt{2\pi}} e^{-\frac{1}{2}\left(\frac{\mu}{\sigma}\right)^2} \quad (65)$$

where Φ_{CDF} is the CDF of a standard univariate Gaussian random variable. In our case, $b \in \mathbb{R}$ (not necessarily positive), and (64) implies that $\mu = -b$ and $\sigma = 1$; whence (65) yields

$$p = \mathbb{E}_{\tilde{\gamma} \sim N(-b,1)}((\text{ReLU}(\tilde{\gamma}))^2) = b^2(1 - \Phi_{CDF}(b)) - \frac{b}{\sqrt{2\pi}} e^{-\frac{b^2}{2}}. \quad (66)$$

Since $g(b) \stackrel{\text{def.}}{=} b^2(1 - \Phi_{CDF}(b)) - \frac{b}{\sqrt{2\pi}} e^{-\frac{b^2}{2}}$ is continuous with $g(0) = 0$ and $\lim_{b \rightarrow -\infty} g(b) = \infty$ then by the intermediate value theorem, a solution to (66) indeed exists. \square

Proposition B.3 (2-Hidden-Layer ReLU Random Feature Model). *Fix sufficiently large integers $F, N \in \mathbb{N}$ such that $F > N^{5(1+\alpha)}$ for some absolute constant $\alpha > 0$. Let $X \in \mathbb{R}^{d \times N}$ with columns $\{x_1, \dots, x_N\} \subset \mathbb{R}^d$ such that*

$$\|x_i\|_2 \in [0, 2], \quad \forall i = 1, \dots, N \text{ and } \|x_i - x_j\|_2 \geq C \sqrt{\frac{(1+\alpha) \log N}{\log F}}, \quad \forall i \neq j$$

for some absolute constant $C > 0$. Let $B^{(1)} \in \mathbb{R}^{F \times d}$ and $B^{(2)} \in \mathbb{R}^{F \times F}$ be random standard Gaussian matrices. Let $p^{(1)}, p^{(2)} > 0$ be given by

$$p^{(1)} \stackrel{\text{def.}}{=} \frac{C \log^2(2NF)}{N^{-2(1+\alpha)} F} \text{ and } p^{(2)} \stackrel{\text{def.}}{=} \frac{1}{\sqrt{F}}.$$

There exist $b^{(1)}, b^{(2)} \in \mathbb{R}$ given implicitly, for $i = 1, 2$, by

$$p^{(i)} = (b^{(i)})^2 (1 - \Phi_{CDF}(b^{(i)})) - \frac{b^{(i)}}{\sqrt{2\pi}} e^{-\frac{(b^{(i)})^2}{2}}.$$

Define the 2-hidden-layer random feature matrix:

$$\begin{aligned} \Psi^{(2)} &= \frac{1}{\sqrt{Fp}} \text{ReLU}(B^{(2)}\Psi^{(1)} + b^{(2)}\mathbf{1}_F\mathbf{1}_F^\top) \in \mathbb{R}^{F \times N} \\ \Psi^{(1)} &= \frac{1}{\sqrt{Fp^{(1)}}} \text{ReLU}(B^{(1)}X + b^{(1)}\mathbf{1}_F\mathbf{1}_N^\top) \in \mathbb{R}^{F \times N}. \end{aligned}$$

Then with probability at least $1 - 2N^{-3-20(1+\alpha)}$ over the draw of $B^{(1)}$ and $B^{(2)}$, the random feature matrix has smallest singular value:

$$\frac{1}{2} - \frac{C_2(1+\alpha) \log^2 N}{N^{1.5+0.5\alpha}} \leq s_{\min}(\Psi_2) \leq s_{\max}(\Psi_2) \leq \frac{1}{2} + \frac{C_2 N \log(F) + \log^2(2F^2)}{\sqrt{F}}. \quad (67)$$

Proof. Analogous to the previous Proposition, we have

$$\Psi^{(1)} = \frac{1}{\sqrt{Fp^{(1)}}} \text{ReLU}(B^{(1)}X + b^{(1)}\mathbf{1}_F\mathbf{1}_N^\top) \in \mathbb{R}^{F \times N}$$

with columns $\psi_i^{(1)}$'s satisfying

$$\left| \|\psi_i^{(1)}\|_2^2 - 1 \right| \leq \varepsilon, \quad \left| \langle \psi_i^{(1)}, \psi_j^{(1)} \rangle \right| \leq \epsilon,$$

where $\varepsilon = N^{-(1+\alpha)}$. Now let $b^2 > 1$ be such that

$$p^{(2)} = \frac{1}{\sqrt{F}} = \mathbb{E}_{\gamma \sim N(0,1)} (\gamma - b^{(2)})^2,$$

and let

$$\Psi^{(2)} = \frac{1}{\sqrt{Fp}} \text{ReLU}(B^{(2)}\Psi^{(1)} + b^{(2)}\mathbf{1}_F\mathbf{1}_F^\top) \in \mathbb{R}^{F \times N}$$

where $B^{(2)} \in \mathbb{R}^{F \times F}$ is a random standard Gaussian matrix. Then apply Lemma C.2 on each pair $\psi_i^{(1)}, \psi_j^{(1)}$ of features: with probability at least $1 - 4F(2F^2)^{-5}$ over the draw of $B^{(2)}$, the columns $\psi_i^{(2)}, \psi_j^{(2)}$ satisfy

$$\|\psi_i^{(2)}\|_2 \geq \frac{1}{2}, \quad \left| \langle \psi_i^{(2)}, \psi_j^{(2)} \rangle \right| \leq \frac{C_2(\log F + \log^2(2F^2))}{\sqrt{F}}$$

By union bound over all pairs and again by Gershgorin Circle Theorem, see e.g. [53, Theorem 6.2.5], with probability at least $1 - 4N^2F(2F^2)^{-5}$ the *smallest* singular value of $\Psi^{(2)}$ is more than

$$\frac{1}{2} - \frac{C_2N(\log F + \log^2(2F^2))}{\sqrt{F}} \geq \frac{1}{2} - \frac{C_2(1+\alpha)\log^2 N}{N^{1.5+0.5\alpha}}$$

where the constant C_2 changes from line to line. By the same stroke, we have that the *largest* singular value of $\Psi^{(2)}$ is at-most

$$\frac{1}{2} + \frac{C_2N \log(F) + \log^2(2F^2)}{\sqrt{F}}$$

still over the draw of $B^{(2)}$. By union bound over the draws of B^1 and $B^{(2)}$ we obtain the result. \square

Proposition B.4 (Well-Conditioning of Deep Feature Matrix). *In the setting of Proposition B.3, let Π be a $(N-1) \times F$ standard Gaussian matrix with i.i.d. $N(0, 1/\sqrt{N-1})$ entries, and consider the **deep feature matrix** \mathbb{X}_Ψ*

$$\mathbb{X}_\Psi \stackrel{\text{def.}}{=} \mathbf{1}_N \oplus ((\Psi^{(2)})^\top \Pi^\top) \in \mathbb{R}^{N \times N}. \quad (68)$$

Then, there are absolute constants $C_2, C > 0$ such that: for N large enough

$$\begin{aligned} \left(\frac{1}{2} - \frac{C_2(1+\alpha)\log^2 N}{N^{(3+\alpha)/2}} \right) (N^{2+\alpha/2} - C) &\leq s_{\min}(\mathbb{X}_\Psi) \\ s_{\max}(\mathbb{X}_\Psi) &\leq \sqrt{\left(C + 2N \log F + \log^2(2F^2) \right)^2 \left(\frac{1}{\sqrt{k}} + \frac{C}{\sqrt{F}} \right)^2 + N^2} \end{aligned} \quad (69)$$

holds with probability at least $1 - 2e^{-N} - 2N^{-3-20(1+\alpha)}$ over the draw of $B^{(1)}$, $B^{(2)}$, and Π .

Proof of Proposition B.4. Since $\tilde{\mathbb{X}}_\Psi \stackrel{\text{def.}}{=} (\Psi^{(2)})^\top \Pi^\top$ is a sub-matrix of \mathbb{X}_Ψ then; a consequence of Weyl's interlacing theorem, see e.g. [53, Corollary 7.3.6], for singular values implies that

$$s_{\min}(\mathbb{X}_\Psi) \geq s_{\min}(\tilde{\mathbb{X}}_\Psi) = s_{\min}((\Psi^{(2)})^\top \Pi^\top) \quad (70)$$

and additionally we have

$$s_{\max}(\mathbb{X}_\Psi) \leq \sqrt{s_{\max}(\tilde{\mathbb{X}}_\Psi)^2 + \|\mathbf{1}_N\|^2} = \sqrt{s_{\max}(\tilde{\mathbb{X}}_\Psi)^2 + N^2} \leq \sqrt{(s_{\max}((\Psi^{(2)})^\top \Pi^\top))^2 + N^2} \quad (71)$$

Abbreviate $k \stackrel{\text{def}}{=} N - 1$. Let $\Pi \stackrel{\text{def}}{=} \frac{1}{\sqrt{N-1}}A$ where A is a $k \times F$ standard random Gaussian matrix. Note that $F \geq N$; thus the $F \times k$ Gaussian matrix A^\top is tall. Thus, by the version of Gordon's Theorem in [109, Theorem 4.6.1] to A^\top , we have that: for all $t > 0$ the following

$$\sqrt{F} - C\sqrt{k} \leq s_{\min}(A^\top) \leq s_{\max}(A^\top) \leq \sqrt{F} + C\sqrt{k} \quad (72)$$

holds with probability at-least $1 - 2e^{-k}$; for some constant $C > 0$ depending only on the sub-Gaussian norm of the rows of A^\top . Since $\Pi = \frac{1}{\sqrt{k}}A$ then

$$s_{\min}(\Pi^\top) = \frac{1}{\sqrt{k}} s_{\min}(A^\top) \geq \frac{\sqrt{F} - C\sqrt{k}}{\sqrt{k}} = \frac{\sqrt{F}}{\sqrt{k}} - C \quad (73)$$

$$s_{\max}(\Pi^\top) = \frac{1}{\sqrt{k}} s_{\max}(A^\top) \leq \frac{\sqrt{F} + C\sqrt{k}}{\sqrt{k}} = \frac{\sqrt{F}}{\sqrt{k}} + C \quad (74)$$

both hold with probability at-least $1 - 2e^{-k}$. In particular, whenever the right-hand side of (73) is bounded away from zero, then Π^\top is of full rank and, in particular, it has linearly independent columns. Recall that, if A and B are matrices such that B has linearly independent columns then¹³ $s_{\min}(AB) \geq s_{\min}(A)s_{\min}(B)$. Consequentially

$$s_{\min}(\Psi^{(2)\top} \Pi^\top) \geq s_{\min}(\Psi^{(2)\top}) s_{\min}(\Pi^\top) \geq s_{\min}(\Psi^{(2)\top}) \left(\frac{\sqrt{F}}{\sqrt{k}} - C \right) \quad (75)$$

holds with probability at-least $1 - 2e^{-N}$.

Now, appealing to Proposition B.3, with probability at least $1 - 2N^{-3-20(1+\alpha)}$ over the draw of $B^{(1)}$ and $B^{(2)}$, the random feature matrix has smallest singular value:

$$s_{\min}(\Psi_2) = s_{\min}(\Psi_2^\top) \geq \frac{1}{2} - \frac{C_2(1+\alpha)\log^2 N}{N^{(3+\alpha)/2}}. \quad (76)$$

Taking a union bound, together (75) and (76) imply that

$$\begin{aligned} s_{\min}(\Psi^{(2)\top} \Pi^\top) &\geq \left(\frac{1}{2} - \frac{C_2(1+\alpha)\log^2 N}{N^{(3+\alpha)/2}} \right) \left(\frac{\sqrt{F}}{\sqrt{k}} - C \right) \\ &\geq \left(\frac{1}{2} - \frac{C_2(1+\alpha)\log^2 N}{N^{(3+\alpha)/2}} \right) \left(\frac{N^{5(1+\alpha)/2}}{N^{1/2}} - C \right) \\ &= \left(\frac{1}{2} - \frac{C_2(1+\alpha)\log^2 N}{N^{(3+\alpha)/2}} \right) (N^{2+\alpha/2} - C) \end{aligned} \quad (77)$$

holds with probability at least $1 - 2e^{-N} - 2N^{-3-20(1+\alpha)}$; where we used the assumption that $F > N^{5(1+\alpha)}$ and the definition of $k = N - 1$ in deriving (77). Now, on the same draw of Π , $B^{(1)}$, and $B^{(2)}$ by (71) and (74) we have that

$$\begin{aligned} s_{\max}(\mathbb{X}_\Psi) &\leq \sqrt{(s_{\max}((\Psi^{(2)})^\top \Pi^\top))^2 + N^2} \\ &\leq \sqrt{s_{\max}((\Psi^{(2)})^2) s_{\max}(\Pi)^2 + N^2} \\ &\leq \sqrt{\left(\frac{C + 2N \log(F) + \log^2(2F^2)}{\sqrt{F}} \right)^2 \left(\frac{\sqrt{F}}{\sqrt{k}} + C \right)^2 + N^2} \\ &= \sqrt{\left(C + 2N \log F + \log^2(2F^2) \right)^2 \left(\frac{1}{\sqrt{k}} + \frac{C}{\sqrt{F}} \right)^2 + N^2}. \end{aligned} \quad (78)$$

where we have applied (76) to bound (78). □

¹³If B has linearly independent columns then $s_{\min}(AB) = \min_{x \neq 0} \frac{\|ABx\|_2}{\|x\|_2} = \min_{x \neq 0} \frac{\|ABx\|_2}{\|Bx\|_2} \frac{\|Bx\|_2}{\|x\|_2} \geq \min_{y \neq 0} \frac{\|Ay\|_2}{\|y\|_2} \min_{x \neq 0} \frac{\|Bx\|_2}{\|x\|_2} = s_{\min}(A)s_{\min}(B)$.

The following shows that the typical operator norm of the regression coefficient $\beta_{\text{OLS}:\mathbb{X},\mathbb{Y}}$ for any (soft-)classification problem of the order of

$$\mathcal{O}\left(\frac{\sqrt{D}\left(\log F\left(\frac{1}{\sqrt{k}} + \frac{1}{\sqrt{F}}\right) + 1\right)}{N^{3+\alpha-1/2}}\right)$$

with high probability, over the over the draw of $B^{(1)}$, $B^{(2)}$, and Π .

Corollary B.1 (Regularity of Regression with Deep Features). *In the setting of Proposition B.4, let $\mathbb{Y} \in \mathbb{R}^{N \times D}$ have all its entries in $[0, 1]$, and consider the deep feature matrix \mathbb{X}_Ψ in (68). Then the solution to the regression problem $\beta_{\text{OLS}:\mathbb{X},\mathbb{Y}}$ (defined in (10)) is well-defined and satisfies*

$$\|\beta_{\text{OLS}:\mathbb{X},\mathbb{Y}}\|_{op} \leq \frac{\sqrt{ND} \sqrt{\left(C + 2N \log F + \log^2(2F^2)\right)^2 \left(\frac{1}{\sqrt{k}} + \frac{C}{\sqrt{F}}\right)^2 + N^2}}{\left[\left(\frac{1}{2} - \frac{C_2(1+\alpha) \log^2 N}{N^{(3+\alpha)/2}}\right) \left(N^{2+\alpha/2} - C\right)\right]^2} \quad (79)$$

holds with probability at least $1 - 2e^{-N} - 2N^{-3-20(1+\alpha)}$ over the draw of $B^{(1)}$, $B^{(2)}$, and Π .

Proof of Corollary B.1. By the Cauchy-Schwarz inequality, we have

$$\begin{aligned} \|\beta\|_{op} &= \|(\mathbb{X}_\Psi^\top \mathbb{X}_\Psi)^{-1} \mathbb{X}_\Psi^\top \mathbb{Y}\|_{op} \\ &\leq \|(\mathbb{X}_\Psi^\top \mathbb{X}_\Psi)^{-1}\|_{op} \|\mathbb{X}_\Psi\|_{op} \|\mathbb{Y}\|_{op} \\ &= \frac{s_{\max}(\mathbb{X}_\Psi)}{s_{\min}(\mathbb{X}_\Psi)^2} \|\mathbb{Y}\|_{op} \\ &\leq \frac{s_{\max}(\mathbb{X}_\Psi)}{s_{\min}(\mathbb{X}_\Psi)^2} \sqrt{ND \max_{i,j} |\mathbb{Y}_{i,j}|} \\ &= \frac{s_{\max}(\mathbb{X}_\Psi)}{s_{\min}(\mathbb{X}_\Psi)^2} \sqrt{ND}. \end{aligned} \quad (80)$$

Now, applying Proposition B.4, the holds with probability at least $1 - 2e^{-N} - 2N^{-3-20(1+\alpha)}$ over the draw of $B^{(1)}$, $B^{(2)}$, and Π

$$\begin{aligned} \|\beta\|_{op} &\leq \frac{s_{\max}(\mathbb{X}_\Psi)}{s_{\min}(\mathbb{X}_\Psi)^2} \sqrt{ND} \\ &\leq \frac{\sqrt{ND} \sqrt{\left(C + 2N \log F + \log^2(2F^2)\right)^2 \left(\frac{1}{\sqrt{k}} + \frac{C}{\sqrt{F}}\right)^2 + N^2}}{\left[\left(\frac{1}{2} - \frac{C_2(1+\alpha) \log^2 N}{N^{(3+\alpha)/2}}\right) \left(N^{2+\alpha/2} - C\right)\right]^2}. \end{aligned}$$

□

B.3 Proof of Main Theorems

Proof of Theorem 5.1. Under our assumptions on N and on q (Assumption 4.1 (i) and (ii)), by Theorem 4.1 we have that with probability at-least $1 - \delta$ (on the draw of \mathcal{D}_τ), $\mathcal{D}_\tau^* = \{x_c, y_c\}_{c=1}^\kappa$ (where for each $c \in \{1, \dots, \kappa\}$ $x_c = \bar{Q}_c$ for some $Q_c \in \mathcal{C}$ and $y_c \stackrel{\text{def.}}{=} \frac{1}{N_Q} \sum_{(X,Y) \in Q} Y_Q$) satisfies

$$\|f(x_c) - y_c\| \leq \varepsilon. \quad (81)$$

On the same draw of \mathcal{D}_τ , Proposition 4.2 implies that the transformed input data $\{u_c\}_{c=1}^\kappa$ defined for each $c = 1, \dots, \kappa$ by

$$u_c \stackrel{\text{def.}}{=} \text{Attn}(x_c | K, V) \quad (82)$$

satisfies the boundedness and separation requirements in (16) (with N replaced by κ). Therefore, under our assumption on F (Assumption 4.1 (iii)) then the conditions of Proposition B.4 of met (for the inputs $\{u_c\}_{c=1}^\kappa$ defined as in (82)); whence the deep design matrix satisfies the well-conditioning guarantee

$$s_{\min}(\mathbb{X}) \geq \left(\frac{1}{2} - \frac{C_2(1+\alpha) \log^2 \kappa}{\kappa^{(3+\alpha)/2}}\right) \left(\kappa^{2+\alpha/2} - C\right) \quad (83)$$

and the boundedness guarantee

$$s_{\max}(\mathbb{X}_\Psi) \leq \sqrt{\left(C + 2\kappa \log F + \log^2(2F^2)\right)^2 \left(\frac{1}{\sqrt{k}} + \frac{C}{\sqrt{F}}\right)^2 + \kappa^2} \quad (84)$$

with probability at least $1 - 2e^{-\kappa} - 2\kappa^{-3-20(1+\alpha)}$. Since (83) holds (on the same draw), then the linear regression problem (20) admits a unique solution. Moreover, the definition of $\beta_{\text{OLS}; \mathbb{X}, \mathbb{Y}}$ (see (10)) and the computations in Corollary 79 yield (21) concluding our proof. Setting $\delta = 1/N$ yields the final conclusion. \square

Proof of Theorem 5.2. Fix $0 < \delta \leq 1$. Since \tilde{N} is greater than or equal to the right-hand side of (11) then: with probability at-least $1 - \delta$

$$\mathbb{P}\left(\max_{Q \in \mathcal{Q}_{\mathbb{P}}} \left\| f(\bar{Q}) - \frac{1}{N_Q} \sum_{(X,Y) \in Q} \tilde{Y}_Q \right\| \leq \varepsilon \right) \geq 1 - \delta. \quad (85)$$

Since the dataset $\mathcal{D}_{\tilde{\tau}}^* \stackrel{\text{def.}}{=} \text{Algo-1}(\mathcal{D}_{\tilde{\tau}}) = \{(\tilde{x}_c, \tilde{y}_c)\}_{c=1}^{\kappa}$ constructed from Algorithm 1 is such that: for each $c \in [\kappa]$

$$x_c \in \cup_{Q \in c} Q \text{ and } y_c = \frac{1}{N_Q} \sum_{(X,Y) \in Q} \tilde{Y}_Q \quad (86)$$

then: with probability at-least $1 - \delta$

$$\mathbb{P}\left(\max_{Q \in \mathcal{Q}_{\mathbb{P}}} \left\| f(\bar{Q}) - y_c \right\| \leq \frac{1}{q} \right) \geq 1 - \delta \quad (87)$$

(where, we emphasize that, the choice $\varepsilon = 1/q$ held by our assumed lower-bound on \tilde{N} in Assumption A.1 (i)). Now, conditional on the success of Theorem 5.1, we know that \mathbb{X} is invertible. Therefore, the system (22) admits a unique solution given by

$$\tilde{\beta}_{\text{OLS}; \mathcal{D}_{\tilde{\tau}}} \stackrel{\text{def.}}{=} (\mathbb{X}^\top \mathbb{X})^\dagger \mathbb{X}^\top \tilde{\mathbb{Y}}$$

with probability at-least $1 - \delta$, conditional on the draw of $\mathcal{D}_{\tilde{\tau}}$. Applying Proposition 4.2 we have that: for every $x \in \mathcal{G}$ and every $c \in [\kappa]$ we have that $x \in \cup_{Q \in c} Q$ if and only if $\text{Attn}(x|K, V) = x_c$. Thus, (86) implies that the fine-tuned transformer $\tilde{f} \stackrel{\text{def.}}{=} \tilde{\beta}_{\text{OLS}; \mathcal{D}_{\tilde{\tau}}} \mathcal{E}$ satisfies

$$\tilde{f}(x) = \tilde{y}_c \quad (88)$$

for all $x \in \mathcal{G}$; again with probability at-least $1 - \delta$ conditional on the draw of $\mathcal{D}_{\tilde{\tau}}$. Now, (88) together with (87) and the ω -uniform continuity of f imply that, with probability at-least $1 - \delta$ conditional on the draw of $\mathcal{D}_{\tilde{\tau}}$, we have that: for every $x \in \mathcal{G}$

$$\begin{aligned} \|f(x) - \tilde{f}(x)\| &\leq \|f(x) - f(x_Q)\| + \|f(x_Q) - y_{c_x}\| + \|y_{c_x} - \tilde{f}(x)\| \\ &= \|f(x) - f(x_Q)\| + \|f(x_Q) - y_{c_x}\| \\ &= \|f(x) - f(x_Q)\| + \frac{1}{q} \end{aligned} \quad (89)$$

$$\leq \omega(\sqrt{d}/q) + \frac{1}{q} \quad (90)$$

where $x_Q \in \text{argmin}_{Q \in \mathcal{Q}_{\mathbb{P}_X}} \|x - \bar{Q}\|_\infty$ and $c_x \in [\kappa]$ is such that $x_Q \in \cup_{Q \in c} Q$; (89) held by (87), and (90) held by the ω -uniform continuity of f and the ℓ^2 -diameter of any cube $Q \in \mathcal{Q}$. Consequently, the following holds with probability at-least $1 - \delta$, conditional on the draw of $\mathcal{D}_{\tilde{\tau}}$,

$$\|f(x) - \tilde{f}(x)\| \leq \omega(\sqrt{d}/q) + \frac{1}{q} \quad (\forall x \in \mathcal{G}). \quad (91)$$

Finally, since $\tilde{\mathbb{P}}_X$ is non-atomic then $\tilde{\mathbb{P}}_X(\mathbb{R}^d \setminus \mathcal{G}) = 0$ whence the essential supremum formulation in (23) follows from (91). \square

We now directly obtain Proposition 5.1 by tweaking the proof of Theorem 5.2.

Proof of Proposition 5.1. Consider the dataset $\{(X_n, Y_n)\}_{n=1}^{\kappa}$ where: for each $n \in [\kappa]$ we let $X_n = \bar{Q}$ for any $Q \in c$ (where $c = n$) and $Y_n = f(\bar{Q})$. Then, the proof of Theorem 5.2 goes through surely (not with probability at-least $1 - \delta$) with $x_n \stackrel{\text{def.}}{=} X_n$ and $y_n \stackrel{\text{def.}}{=} Y_n$ at step (87); additionally, note that the extra additive error of $1/q$ can be omitted here since, by construction, (87) is replaced by $\|f(\bar{Q}) - y_c\| = 0$. \square

C Technical Lemmata

This section contains additional technical lemmata, largely from what is sometimes loosely called “non-linear random matrix theory”, used in deriving our main results.

C.1 Non-Linear Random Matrices

Proposition C.1 (Relaxed version of Prop. 3.1 in [110]). *Let $x, x' \in \mathbb{R}^n$ satisfy*

$$\|x\|_2, \|x'\|_2 \in [1 - \epsilon, 1 + \epsilon] \quad \text{for some } 0 \leq \epsilon < 1.$$

Assume $b > 1$, and let $g \sim \mathcal{N}(0, I_n)$ be a standard Gaussian vector. Then for either the threshold or the ReLU nonlinearity ϕ , we have

$$\mathbb{E}[\phi(\langle g, x \rangle - b) \phi(\langle g, x' \rangle - b)] \leq C \exp(-b^2 \|x - x'\|_2^2 / 8) \mathbb{E}[\phi(\gamma - b)^2],$$

where $C > 0$ is an absolute constant for $b \in \mathbb{R}$.

Proof of Proposition C.1. We follow the original three-step argument from the unit-norm case, modifying each step to handle $\|x\|_2, \|x'\|_2 \in [1 - \epsilon, 1 + \epsilon]$.

Step 1 (Orthogonal decomposition). Define

$$u = \frac{x + x'}{2}, \quad v = \frac{x - x'}{2}.$$

Then $x = u + v$ and $x' = u - v$. We claim that for any $z \in \mathbb{R}^n$,

$$\phi(\langle z, x \rangle - b) \phi(\langle z, x' \rangle - b) \leq [\phi(\langle z, u \rangle - b)]^2. \quad (92)$$

Indeed, if both $\langle z, x \rangle$ and $\langle z, x' \rangle$ exceed b , then $\langle z, u \rangle$ must also exceed b . For threshold $\phi(t) = \mathbf{1}_{\{t > 0\}}$, this yields

$$\mathbf{1}_{\{\langle z, x \rangle > b\}} \mathbf{1}_{\{\langle z, x' \rangle > b\}} \leq \mathbf{1}_{\{\langle z, u \rangle > b\}},$$

implying (92). For ReLU $\phi(t) = \max(0, t)$, one also uses $(\langle z, x \rangle - b)(\langle z, x' \rangle - b) \leq (\langle z, u \rangle - b)^2$ whenever both $\langle z, x \rangle, \langle z, x' \rangle > b$, arriving at the same conclusion.

Step 2 (Taking expectation). Let $g \sim \mathcal{N}(0, I_n)$. By setting $z = g$ in (92) and taking expectation on both sides,

$$\mathbb{E}[\phi(\langle g, x \rangle - b) \phi(\langle g, x' \rangle - b)] \leq \mathbb{E}[\phi(\langle g, u \rangle - b)^2].$$

Note that

$$u = \frac{x + x'}{2}, \quad v = \frac{x - x'}{2}, \quad \delta = \|v\|_2 = \frac{1}{2} \|x - x'\|_2.$$

Accordingly,

$$\|u\|_2^2 = \frac{\|x\|_2^2 + \|x'\|_2^2}{2} - \|v\|_2^2 \in [(1 - \epsilon)^2 - \delta^2, (1 + \epsilon)^2 - \delta^2].$$

Set $r = \|u\|_2^2$. Then $\langle g, u \rangle$ is $\mathcal{N}(0, r)$, so

$$\mathbb{E}[\phi(\langle g, u \rangle - b)^2] = \mathbb{E}[\phi(\sqrt{r} \gamma - b)^2], \quad \text{where } \gamma \sim \mathcal{N}(0, 1).$$

Thus

$$\mathbb{E}[\phi(\langle g, x \rangle - b) \phi(\langle g, x' \rangle - b)] \leq \mathbb{E}[\phi(\sqrt{r} \gamma - b)^2], \quad r \in [(1 - \epsilon)^2 - \delta^2, (1 + \epsilon)^2 - \delta^2]. \quad (93)$$

Note that $0 \leq \delta^2 \leq (1 + \epsilon)^2 < 2$.

Step 3 (Stability). Choose

$$r_{\max} := (1 + \epsilon)^2 - \delta^2, \quad \text{so } 0 \leq r \leq r_{\max} \leq 2 - \delta^2.$$

Then

$$\mathbb{E}[\phi(\sqrt{r} \gamma - b)^2] \leq \mathbb{E}[\phi(\sqrt{r_{\max}} \gamma - b)^2] = \mathbb{E}[\phi(\sqrt{1 + z} \gamma - b)^2]$$

where we write $r_{\max} = 1 + z$, i.e.

$$z = r_{\max} - 1 = (1 + \epsilon)^2 - 1 - \delta^2 = 2\epsilon + \epsilon^2 - \delta^2 \geq -1.$$

We now apply a normal “stability” inequality (cf. Lemma A.2 in [110]): for sufficiently large $b > 1$, there exist absolute constants such that

$$\frac{\mathbb{E}[\phi(\sqrt{1+z}\gamma - b)^2]}{\mathbb{E}[\phi(\gamma - b)^2]} \leq C \exp\left(\frac{b^2 z}{2(1+z)}\right) (1+z)^{3/2} \leq C \exp\left(-\frac{b^2(-z)}{2}\right)$$

where C is some absolute constant for $b > 1$. As $\delta = \frac{1}{2}\|x - x'\|_2$, we have

$$\mathbb{E}[\phi(\sqrt{r_{\max}}\gamma - b)^2] \leq C e^{2\epsilon} \exp(-b^2 \|x - x'\|_2^2 / 8) \mathbb{E}[\phi(\gamma - b)^2],$$

and combining with (93) we finally get

$$\mathbb{E}[\phi(\langle g, x \rangle - b) \phi(\langle g, x' \rangle - b)] \leq C e^{2\epsilon} \exp(-b^2 \|x - x'\|_2^2 / 8) \mathbb{E}[\phi(\gamma - b)^2].$$

Replacing $C e^{2\epsilon}$ by a larger absolute constant, we obtain the desired result. \square

Lemma C.1 (Enrichment I: from separated to ε -orthogonal, relaxed norms). *Let $x, x' \in \mathbb{R}^n$ satisfy*

$$\|x\|_2, \|x'\|_2 \in [0, 2], \quad \|x - x'\|_2 \geq C_2 \sqrt{\frac{\log(\frac{1}{\varepsilon})}{\log m}},$$

for some $\varepsilon \in [m^{-1/5}, \frac{1}{8}]$, and a sufficiently large absolute constant $C_2 > 0$. Suppose $2 \leq N \leq \exp(m^{1/5})$.

Define real numbers p and $b > 1$ so that

$$p = \frac{C_2 \log^2 N}{\varepsilon^2 m} = \mathbb{E}[\phi(\gamma - b)^2], \quad \text{where } \gamma \sim \mathcal{N}(0, 1), \quad \phi(t) \in \{\mathbf{1}_{\{t > 0\}}, \max(0, t)\}.$$

Let $g_1, \dots, g_m \sim \mathcal{N}(0, I_n)$ be independent standard Gaussians, and define the random map

$$\Phi : \mathbb{R}^n \rightarrow \mathbb{R}^m, \quad \Phi(x) := \left(\phi(\langle g_i, x \rangle - b) \right)_{i=1}^m.$$

Then, with probability at least $1 - 4m N^{-5}$, the vectors

$$u := \frac{\Phi(x)}{\sqrt{mp}} \quad \text{and} \quad u' := \frac{\Phi(x')}{\sqrt{mp}}$$

satisfy

$$\left| \|u\|_2^2 - 1 \right| \leq \varepsilon, \quad \text{and} \quad |\langle u, u' \rangle| \leq \varepsilon.$$

Proof. We follow the same three-step argument as the original Lemma 5.1 in [110], but now relying on the relaxed Proposition C.1 that accommodates $\|x\|_2, \|x'\|_2 \in [1 - 1, 1 + 1]$. \square

Lemma C.2 (Enrichment II: from ε -orthogonal to $1/\sqrt{d}$ -orthogonal). *Let $u, u' \in \mathbb{R}^m$ satisfy*

$$\left| \|u\|_2^2 - 1 \right| \leq \varepsilon, \quad \left| \|u'\|_2^2 - 1 \right| \leq \varepsilon, \quad |\langle u, u' \rangle| \leq \varepsilon,$$

for some $\varepsilon \in (0, c/\log d)$ that is sufficiently small. Let $g_1, \dots, g_d \sim \mathcal{N}(0, I_m)$ be independent standard Gaussian vectors in \mathbb{R}^m , and define a random map

$$\Phi : \mathbb{R}^m \rightarrow \mathbb{R}^d, \quad \Phi(z) = [\phi(\langle g_i, z \rangle - b)]_{i=1}^d$$

where ϕ is either the threshold activation $\mathbf{1}_{\{t > 0\}}$ or the ReLU activation $t \mapsto \max(0, t)$, and $b \in \mathbb{R}$ is chosen so that

$$\mathbb{E}[\phi(\gamma - b)^2] = p = \frac{1}{\sqrt{d}}, \quad \text{with } \gamma \sim \mathcal{N}(0, 1).$$

Set

$$v = \frac{\Phi(u)}{\sqrt{d}p} \quad \text{and} \quad v' = \frac{\Phi(u')}{\sqrt{d}p}.$$

Then, with probability at least $1 - 4dN^{-5}$ with $\exp(c d^{1/5}) \geq N \geq 2$, the following two properties hold:

$$\|v\|_2 \geq \frac{1}{2} \quad \text{and} \quad |\langle v, v' \rangle| \leq C \frac{\log(dN)}{\sqrt{d}},$$

for absolute constants $c, C > 0$.

Theorem C.1 (Enrichment I: from separated to ε_0 -orthogonal, relaxed norms). *Let $x_1, \dots, x_K \in \mathbb{R}^n$ satisfy*

$$\|x_i\|_2 \in [1 - \epsilon, 1 + \epsilon], \quad \|x_i - x_j\|_2 \geq C_2 \sqrt{\frac{\log(\frac{1}{\varepsilon_0})}{\log m}} \quad \text{for all distinct } i, j,$$

where $\epsilon \in [0, 1)$, $\varepsilon_0 \in [m^{-1/5}, \frac{1}{8}]$, and $C_2 > 0$ is a sufficiently large absolute constant. Assume also that

$$K \leq \exp(c_2 m^{1/5})$$

for some absolute constant $c_2 > 0$.

Then with probability at least $1 - \frac{1}{8m^4K^3}$, the almost pseudolinear map $E : \mathbb{R}^n \rightarrow \mathbb{R}^m$ such that the vectors

$$u_i := E(x_i) \quad (1 \leq i \leq K)$$

satisfy

$$|\|u_i\|_2^2 - 1| \leq \varepsilon_0, \quad |\langle u_i, u_j \rangle| \leq \varepsilon_0 \quad \text{for all distinct } i, j = 1, \dots, K.$$

“Almost pseudolinear” means $E = \lambda\Phi$ for some $\lambda \geq 0$ and a genuine pseudolinear map Φ . In particular, E can be realized by one layer of neurons having Threshold or ReLU activation.

Theorem C.2 (Enrichment II: from ε_0 -orthogonal to $O(\frac{1}{\sqrt{d}})$ -orthogonal). *Let $u_1, \dots, u_K \in \mathbb{R}^m$ satisfy*

$$|\|u_i\|_2^2 - 1| \leq \varepsilon_0 \quad \text{and} \quad |\langle u_i, u_j \rangle| \leq \varepsilon_0 \quad \text{for all distinct } i, j,$$

where $0 < \varepsilon_0 \leq c_3/\log d$ and $K \leq \exp(c_3 d^{1/5})$ for an absolute constant $c_3 > 0$. Then there exists an almost pseudolinear map $R : \mathbb{R}^m \rightarrow \mathbb{R}^d$ such that the vectors

$$v_i := R(u_i) \quad (1 \leq i \leq K)$$

satisfy

$$\|v_i\|_2 \geq \frac{1}{2}, \quad |\langle v_i, v_j \rangle| \leq C_4 \frac{\log^2(dK)}{\sqrt{d}} \quad \text{for all distinct } i, j.$$

Moreover, R can be realized by one layer of neurons with Threshold or ReLU activation.

D Symmetries and Smoothness are Not Related

We now prove that there is no relationship between the number of symmetries a function can have and its degree of smoothness, as quantified by the maximum number of continuous partial derivatives it admits. The following is a more technical version of Proposition 3.2.

Proposition D.1 (Construction of Symmetric Function with Prescribed Smoothness and Values). *Let $d, D, q, K \in \mathbb{N}_+$ with $1 \leq K \leq q^d$ and let $\varepsilon > 0$. For every smoothness level $s \in \mathbb{N}_+$ and every set of ε -separated vectors $\beta_{OLS:\cdot} \stackrel{\text{def}}{=} \{\beta_k\}_{k=1}^K$ there exists a K -symmetric function at scale q for which:*

(i) **Perscribed Smoothness:** $f_{\beta_{OLS:\cdot}}$ all continuous partial derivatives up to order s , but not up to order $s + 1$,

(ii) **Superscribed Range:** $f_{\beta_{OLS:\cdot}}(\{\bar{Q}\}_{Q \in \mathcal{Q}_q}) = \{\beta_k\}_{k=1}^K$.

Proof of Proposition D.1. Let $s \in \mathbb{N}_+$ and consider the elementary “unnormalized bump-like” function $\tilde{\psi}^s : \mathbb{R} \rightarrow [0, \infty)$ given for any $u \in \mathbb{R}$ by

$$\tilde{\psi}^s(u) \stackrel{\text{def.}}{=} \text{ReLU}^s \left(-\text{ReLU}^s(2x + 1/2) - \text{ReLU}^s(-2x + 1/2) + 2 \right).$$

Note that $\tilde{\psi}^s(0) > 0$ for all $s \geq 1$. Observe also that the $(s-1)^{\text{rst}}$ derivative of $\tilde{\psi}$ is continuous and piecewise linear; whence, $\tilde{\psi}^s$ is s -times, but not $s+1$ times, continuously differentiable. Define the multivariate normalized “bump function” $\psi^s : \mathbb{R}^d \rightarrow [0, 1]$ by

$$\psi^s(u) \stackrel{\text{def.}}{=} \prod_{i=1}^d \frac{\tilde{\psi}^s(x_i)}{\tilde{\psi}^s(0)}.$$

Therefore, by construction, ψ^s is in $C^s(\mathbb{R}^d, \mathbb{R}) \setminus C^{s+1}(\mathbb{R}^d, \mathbb{R})$, its support is contained in $[-1, 1]^d$, and $\psi^s(0) = 1$.

Now, fix a number of symmetries $K \in \mathbb{N}_+$ and a K -combinatorial symmetry at scale q , $\mathcal{S} : \mathcal{Q}_q \rightarrow [K]$. Recall the symmetry classes $\{\mathcal{S}_k\}_{k=1}^K$ by

$$\mathcal{S}_k \stackrel{\text{def.}}{=} \{Q \in \mathcal{Q} : \mathcal{S}(Q) = k\}$$

for $k \in [K]$. For any set of ε -separated “values” $\beta_{\text{OLS}..} \stackrel{\text{def.}}{=} \{\beta_k\}_{k=1}^K \in \mathbb{R}^D$ induces a function an $(\varepsilon, \mathcal{S})$ -symmetric function $f_{\beta_{\text{OLS}..}}$ by

$$f_{\beta_{\text{OLS}..}}(x) \stackrel{\text{def.}}{=} \sum_{Q \in \mathcal{Q}_q} \underbrace{\psi^s\left(\frac{1}{2q}(x - \bar{Q})\right)}_{x \text{ belongs to cube } Q?} \underbrace{\sum_{k=1}^K \beta_k I_{Q \in \mathcal{S}_k}}_{x \text{ belongs to symmetry set } \mathcal{S}_k?}$$

where $x \in \mathbb{R}^d$. By construction, we have

$$f_{\beta_{\text{OLS}..}} \in \overbrace{\mathcal{S}_{q,\varepsilon}([0, 1]^d, \mathbb{R}^D)}^{\text{Symmetries}} \cap \overbrace{C^s(\mathbb{R}^d, \mathbb{R}^D) \setminus C^{s+1}(\mathbb{R}^d, \mathbb{R}^D)}^{\text{Exactly Regularity}}.$$

This concludes our construction and, therefore, our proof. \square

D.1 Proofs For Motivational Results for Symmetries

Proof of Proposition 3.1. The first conclusion follows from the integrability of f and the Pigeonhole principle. For the more refined version, by Van der Waerden’s theorem we know that there must be a minimal natural number $W(\hbar, k)$ such that every map from $[W(\hbar, k)] \stackrel{\text{def.}}{=} \{n \in \mathbb{N} : n \leq W(\hbar, k)\}$ to $[\hbar]$ must be such that least one “colour” $r \in [\hbar]$ is repeated k times; by Gower’s version of the result given in [49, Theorem 18.2] we have the (seemingly large but standard in Ramsey theory) bound

$$W(\hbar, k) \leq 2^{2^{\hbar} 2^{2k+9}}. \quad (94)$$

If we take q to be large enough, so that $2^{2^{\hbar} 2^{2k+9}} \leq q^d$, i.e. $2^{\frac{2}{d} \hbar 2^{2k+9}} \leq q$ then, there exists value (“colour”) $r \in [\hbar]$ which is repeated at-least k times. \square

We include the following simple result showing that: the centre value of the coarsened function is very close to that of the concourse function, for large values of q and \hbar , if f is continuous on $[0, 1]^d$. As remarked by the following simple computation, the coarsened function approximates the value of the original function at the centre of each cube while restricting the possible “wiggles” it can take.

Proposition D.2 (Representative of Midpoint of Averaged Function). *Let $q, \hbar, k \in \mathbb{N}_+$. If, moreover ω be a modulus of continuity for $f : [0, 1]^d \rightarrow \mathbb{R}$, then $\max_{Q \in \mathcal{Q}} \sup_{x \in Q, \|x - \bar{Q}\|_\infty \leq 1/2^{h+1}} |f_{q,\hbar}(x) - f(\bar{Q})| \leq \omega\left(\frac{\sqrt{d}}{q}\right) + \frac{1}{\hbar}$.*

Proof of Proposition D.2. First fix an arbitrary cube $Q \in \mathcal{Q}$, by the Lebesgue Differentiation Theorem, see [67], if f is ω -uniformly continuous (and thus $L^1_{loc}(\mathbb{R}^d)$) any any $x \in Q$ with $\|x - \bar{Q}\|_\infty \leq \frac{1}{2^{h+1}}$ by definition of $f_{q,\hbar}$ (see (9))

and of the averaging operator $A_{Q,h}$ (see (8)) we have

$$\left| f_{q,l}(x) - f(\bar{Q}) \right| = \left| A_{Q,l}(x) - f(\bar{Q}) \right| \quad (95)$$

$$\begin{aligned} &\leq \left| \frac{1}{|Q|} \int_Q f(x) dx - A_{Q,l}(x) \right| + \left| \frac{1}{|Q|} \int_Q f(x) dx - f(\bar{Q}) \right| \\ &\leq \frac{1}{h} + \frac{1}{|Q|} \left| \int_Q f(x) dx - f(\bar{Q}) \right| dx. \end{aligned} \quad (96)$$

Now, by the uniform continuity of f we deduce that

$$\left| \frac{1}{|Q|} \int_Q f(x) dx - f(\bar{Q}) \right| \leq \frac{\omega(\text{diam}(Q))}{|Q|} \left| \int_Q 1 dx \right| dx \quad (97)$$

$$\begin{aligned} &= \omega(\text{diam}(Q)) \\ &= \omega\left(\frac{\sqrt{d}}{q}\right). \end{aligned} \quad (98)$$

Now, combining (95)-(96) with (97)-(98) we obtain the conclusion. \square

References

- [1] Ahmed Abdeljawad and Thomas Dittrich. Weighted Sobolev Approximation Rates for Neural Networks on Unbounded Domains. arXiv preprint arXiv:2411.04108, 2024.
- [2] Beatrice Acciaio, Anastasis Kratsios, and Gudmund Pammer. Designing universal causal deep learning models: The geometric (hyper) transformer. Mathematical Finance, 34(2):671–735, 2024.
- [3] Radhakrishna Achanta, Appu Shaji, Kevin Smith, Aurélien Lucchi, Pascal Fua, and Sabine Süsstrunk. Slic superpixels compared to state-of-the-art superpixel methods. IEEE Transactions on Pattern Analysis and Machine Intelligence, 34(11):2274–2282, 2012.
- [4] Ben Adcock, Simone Brugiapaglia, Nick Dexter, and Sebastian Moraga. Deep neural networks are effective at learning high-dimensional hilbert-valued functions from limited data. arXiv preprint arXiv:2012.06081, 2020.
- [5] Noga Alon, Shai Ben-David, Nicolo Cesa-Bianchi, and David Haussler. Scale-sensitive dimensions, uniform convergence, and learnability. Journal of the ACM (JACM), 44(4):615–631, 1997.
- [6] Noga Alon, Shai Ben-David, Nicolò Cesa-Bianchi, and David Haussler. Scale-sensitive dimensions, uniform convergence, and learnability. J. ACM, 44(4):615–631, 1997.
- [7] Pierre Alquier, James Ridgway, and Nicolas Chopin. On the properties of variational approximations of gibbs posteriors. Journal of Machine Learning Research, 17(236):1–41, 2016.
- [8] Luigi Ambrosio. Some fine properties of sets of finite perimeter in ahlfors regular metric measure spaces. Advances in Mathematics, 159(1):51–67, 2001.
- [9] Maria-Florina Balcan and Avrim Blum. On a theory of learning with similarity functions. In Proceedings of the 23rd international conference on Machine learning, pages 73–80, 2006.
- [10] Andrew R Barron. Universal approximation bounds for superpositions of a sigmoidal function. IEEE Transactions on Information theory, 39(3):930–945, 1993.
- [11] Peter L Bartlett, Dylan J Foster, and Matus J Telgarsky. Spectrally-normalized margin bounds for neural networks. Advances in neural information processing systems, 30, 2017.
- [12] Peter L Bartlett, Nick Harvey, Christopher Liaw, and Abbas Mehrabian. Nearly-tight vc-dimension and pseudodimension bounds for piecewise linear neural networks. Journal of Machine Learning Research, 20(63):1–17, 2019.

- [13] Peter L Bartlett and Wolfgang Maass. Vapnik-chervonenkis dimension of neural nets. The handbook of brain theory and neural networks, pages 1188–1192, 2003.
- [14] Maxime Beauchamp. On numerical computation for the distribution of the convolution of N independent rectified Gaussian variables. J. SfdS, 159(1):88–111, 2018.
- [15] Anselm Blumer, Andrzej Ehrenfeucht, David Haussler, and Manfred K Warmuth. Learnability and the vapnik-chervonenkis dimension. Journal of the ACM (JACM), 36(4):929–965, 1989.
- [16] Helmut Bolcskei, Philipp Grohs, Gitta Kutyniok, and Philipp Petersen. Optimal approximation with sparsely connected deep neural networks. SIAM Journal on Mathematics of Data Science, 1(1):8–45, 2019.
- [17] Simone Brugiapaglia. Practical existence theorems for deep learning approximation in high dimensions. In 15th International Conference on Sampling Theory and Applications, 2024.
- [18] Simone Brugiapaglia, Nick Dexter, Samir Karam, and Weiqi Wang. Physics-informed deep learning and compressive collocation for high-dimensional diffusion-reaction equations: practical existence theory and numerics. arXiv preprint arXiv:2406.01539, 2024.
- [19] Shengze Cai, Zhiping Mao, Zhicheng Wang, Minglang Yin, and George Em Karniadakis. Physics-informed neural networks (pinns) for fluid mechanics: A review. Acta Mechanica Sinica, 37(12):1727–1738, 2021.
- [20] Hong-Bin Chen, Sinho Chewi, and Jonathan Niles-Weed. Dimension-free log-sobolev inequalities for mixture distributions. Journal of Functional Analysis, 281(11):109236, 2021.
- [21] Tin Sum Cheng, Aurelien Lucchi, Anastasis Kratsios, and David Belius. Characterizing overfitting in kernel ridgeless regression through the eigenspectrum. In Ruslan Salakhutdinov, Zico Kolter, Katherine Heller, Adrian Weller, Nuria Oliver, Jonathan Scarlett, and Felix Berkenkamp, editors, Proceedings of the 41st International Conference on Machine Learning, volume 235 of Proceedings of Machine Learning Research, pages 8141–8162. PMLR, 21–27 Jul 2024.
- [22] Tin Sum Cheng, Aurelien Lucchi, Anastasis Kratsios, and David Belius. A comprehensive analysis on the learning curve in kernel ridge regression. Advances in Neural Information Processing Systems, 37:24659–24723, 2024.
- [23] Tin Sum Cheng, Aurelien Lucchi, Anastasis Kratsios, Ivan Dokmanić, and David Belius. A theoretical analysis of the test error of finite-rank kernel ridge regression. In Thirty-seventh Conference on Neural Information Processing Systems, 2023.
- [24] Patrick Cheridito, Arnulf Jentzen, and Florian Rossmannek. Efficient approximation of high-dimensional functions with neural networks. IEEE Transactions on Neural Networks and Learning Systems, 33(7):3079–3093, 2021.
- [25] Albert Cohen, Ronald DeVore, Guergana Petrova, and Przemysław Wojtaszczyk. Optimal stable nonlinear approximation. Foundations of Computational Mathematics, 22(3):607–648, 2022.
- [26] Roberto Colomboni, Emmanuel Esposito, and Andrea Paudice. An improved uniform convergence bound with fat-shattering dimension. Information Processing Letters, 188:106539, 2025.
- [27] Salvatore Cuomo, Vincenzo Schiano Di Cola, Fabio Giampaolo, Gianluigi Rozza, Maziar Raissi, and Francesco Piccialli. Scientific machine learning through physics-informed neural networks: Where we are and what’s next. Journal of Scientific Computing, 92(3):88, 2022.
- [28] George Cybenko. Approximation by superpositions of a sigmoidal function. Mathematics of Control, Signals and Systems, 2(4):303–314, 1989.
- [29] Ingrid Daubechies, Ronald DeVore, Simon Foucart, Boris Hanin, and Guergana Petrova. Nonlinear approximation and (deep) relu networks. Constructive Approximation, 55(1):127–172, 2022.
- [30] Giovanni Dematteis, Tobias Grafke, and Eric Vanden-Eijnden. Rogue waves and large deviations in deep sea. Proceedings of the National Academy of Sciences, 115(5):855–860, 2018. Large-deviation and extreme value analysis for rare rogue-wave events in ocean dynamics.

- [31] Ronald A. DeVore. Nonlinear approximation. In Acta numerica, 1998, volume 7 of Acta Numer., pages 51–150. Cambridge Univ. Press, Cambridge, 1998.
- [32] Ronald A DeVore, George Kyriazis, Dany Leviatan, and Vladimir M Tikhomirov. Wavelet compression and nonlinear n-widths. Adv. Comput. Math., 1(2):197–214, 1993.
- [33] Ilias Diakonikolas, Daniel M Kane, and Alistair Stewart. Learning multivariate log-concave distributions. In Conference on Learning Theory, pages 711–727. PMLR, 2017.
- [34] Sjoerd Dirksen, Patrick Finke, and Martin Genzel. Memorization with neural nets: Going beyond the worst case. Journal of Machine Learning Research, 25(347):1–38, 2024.
- [35] Gintare Karolina Dziugaite and Daniel M Roy. Computing nonvacuous generalization bounds for deep (stochastic) neural networks with many more parameters than training data. arXiv preprint arXiv:1703.11008, 2017.
- [36] Giuseppe Alessio D’Inverno, Monica Bianchini, and Franco Scarselli. Vc dimension of graph neural networks with pfaian activation functions. Neural Networks, 182:106924, 2025.
- [37] Ayoub El Hanchi, Chris J Maddison, and Murat A Erdogdu. On the efficiency of erm in feature learning. Advances in Neural Information Processing Systems, 37:98596–98624, 2024.
- [38] Paul Embrechts, Claudia Klüppelberg, and Thomas Mikosch. Modelling Extremal Events: for Insurance and Finance. Springer, 1997. Foundational text bridging EVT and finance/insurance.
- [39] Alireza Fathollah Pour and Hassan Ashtiani. Benefits of additive noise in composing classes with bounded capacity. Advances in Neural Information Processing Systems, 35:32709–32722, 2022.
- [40] Oisín Faust and Hamza Fawzi. Sum-of-squares proofs of logarithmic sobolev inequalities on finite markov chains. IEEE Transactions on Information Theory, 70(2):803–819, 2023.
- [41] Pedro F Felzenszwalb and Daniel P Huttenlocher. Efficient graph-based image segmentation. International Journal of Computer Vision, 59(2):167–181, 2004.
- [42] Sally Floyd and Manfred Warmuth. Sample compression, learnability, and the vapnik-chervonenkis dimension. Machine learning, 21(3):269–304, 1995.
- [43] Nicola Rares Franco and Simone Brugiapaglia. A practical existence theorem for reduced order models based on convolutional autoencoders. Foundations of Data Science, 7(1):72–98, 2025.
- [44] Spencer Frei, Niladri S Chatterji, and Peter Bartlett. Benign overfitting without linearity: Neural network classifiers trained by gradient descent for noisy linear data. In Conference on Learning Theory, pages 2668–2703. PMLR, 2022.
- [45] Ken-Ichi Funahashi. On the approximate realization of continuous mappings by neural networks. Neural networks, 2(3):183–192, 1989.
- [46] Mario Geiger, Stefano Spigler, Stephane d’Ascoli, Levent Sagun, Giulio Biroli, and Matthieu Wyart. Scaling description of generalization with number of parameters in deep learning. In International Conference on Machine Learning, pages 3647–3657. PMLR, 2020.
- [47] Lukas Gonon. Random feature neural networks learn black-scholes type pdes without curse of dimensionality. Journal of Machine Learning Research, 24(189):1–51, 2023.
- [48] Lukas Gonon, Lyudmila Grigoryeva, and Juan-Pablo Ortega. Risk bounds for reservoir computing. Journal of Machine Learning Research, 21(240):1–61, 2020.
- [49] William T Gowers. A new proof of szemerédi’s theorem. Geometric & Functional Analysis GAFA, 11(3):465–588, 2001.
- [50] Boris Hanin. Universal function approximation by deep neural nets with bounded width and relu activations. Mathematics, 7(10):992, 2019.

- [51] Wassily Hoeffding. Probability inequalities for sums of bounded random variables. J. Amer. Statist. Assoc., 58:13–30, 1963.
- [52] Ruiyang Hong and Anastasis Kratsios. Bridging the gap between approximation and learning via optimal approximation by relu mlps of maximal regularity. arXiv preprint arXiv:2409.12335, 2024.
- [53] Roger A. Horn and Charles R. Johnson. Matrix analysis. Cambridge University Press, Cambridge, second edition, 2013.
- [54] Kurt Hornik, Maxwell Stinchcombe, and Halbert White. Multilayer feedforward networks are universal approximators. Neural Networks, 2(5):359–366, 1989.
- [55] Kurt Hornik, Maxwell Stinchcombe, and Halbert White. Universal approximation of an unknown mapping and its derivatives using multilayer feedforward networks. Neural networks, 3(5):551–560, 1990.
- [56] Songyan Hou, Parnian Kassaie, Anastasis Kratsios, Andreas Krause, and Jonas Rothfuss. Instance-dependent generalization bounds via optimal transport. Journal of Machine Learning Research, 24(349):1–51, 2023.
- [57] Jason Hu, Bowen Song, Xiaojian Xu, Liyue Shen, and Jeffrey A Fessler. Learning image priors through patch-based diffusion models for solving inverse problems. Advances in Neural Information Processing Systems, 37:1625–1660, 2024.
- [58] Arthur Jacot, Franck Gabriel, and Clément Hongler. Neural tangent kernel: Convergence and generalization in neural networks. In Advances in Neural Information Processing Systems (NeurIPS), volume 31, 2018.
- [59] Yuling Jiao, Yanming Lai, Xiliang Lu, Fengru Wang, Jerry Zhijian Yang, and Yuanyuan Yang. Deep neural networks with relu-sine-exponential activations break curse of dimensionality in approximation on hölder class. SIAM Journal on Mathematical Analysis, 55(4):3635–3649, 2023.
- [60] Patrick Kidger and Terry Lyons. Universal approximation with deep narrow networks. In Conference on learning theory, pages 2306–2327. PMLR, 2020.
- [61] Junghwan Kim, Michelle Kim, and Barzan Mozafari. Provable memorization capacity of transformers. In The Eleventh International Conference on Learning Representations, 2023.
- [62] Yiwen Kou, Zixiang Chen, Yuanzhou Chen, and Quanquan Gu. Benign overfitting in two-layer relu convolutional neural networks. In International conference on machine learning, pages 17615–17659. PMLR, 2023.
- [63] Nikola Kovachki, Zongyi Li, Burigede Liu, Kamyar Azizzadenesheli, Kaushik Bhattacharya, Andrew Stuart, and Anima Anandkumar. Neural operator: Learning maps between function spaces with applications to pdes. Journal of Machine Learning Research, 24(89):1–97, 2023.
- [64] Anastasis Kratsios, Valentin Debarnot, and Ivan Dokmanić. Small transformers compute universal metric embeddings. Journal of Machine Learning Research, 24(170):1–48, 2023.
- [65] Anastasis Kratsios and Takashi Furuya. Is in-context universality enough? mlps are also universal in-context. arXiv preprint arXiv:2502.03327, 2025.
- [66] Anastasis Kratsios and Léonie Papon. Universal approximation theorems for differentiable geometric deep learning. Journal of Machine Learning Research, 23(196):1–73, 2022.
- [67] Henri Lebesgue. Sur l’intégration des fonctions discontinues. In Annales scientifiques de l’École normale supérieure, volume 27, pages 361–450, 1910.
- [68] Johannes Lederer, Lu Yu, and Irina Gaynanova. Oracle inequalities for high-dimensional prediction. Bernoulli, 25(2):1225–1255, 2019.
- [69] Michel Ledoux and Michel Talagrand. Probability in Banach spaces, volume 23 of Ergebnisse der Mathematik und ihrer Grenzgebiete (3) [Results in Mathematics and Related Areas (3)]. Springer-Verlag, Berlin, 1991. Isoperimetry and processes.
- [70] Wee Sun Lee, Peter L Bartlett, and Robert C Williamson. Lower bounds on the vc-dimension of smoothly parametrized function classes. In Proceedings of the seventh annual conference on Computational learning theory, pages 362–367, 1994.

- [71] Yannick Limmer, Anastasis Kratsios, Xuwei Yang, Raeid Saqur, and Blanka Horvath. Higher-order transformer derivative estimates for explicit pathwise learning guarantees. arXiv preprint arXiv:2405.16563, 2024.
- [72] Min Lin, Qiang Chen, and Shuicheng Yan. Network in network. arXiv preprint arXiv:1312.4400, 2013.
- [73] Nick Littlestone and Manfred Warmuth. Relating data compression and learnability, 1986.
- [74] George G Lorentz, Manfred von Golitschek, and Yuly Makovoz. Constructive approximation: advanced problems, volume 304. Citeseer, 1996.
- [75] Jianfeng Lu, Zuowei Shen, Haizhao Yang, and Shijun Zhang. Deep network approximation for smooth functions. SIAM J. Math. Anal., 53(5):5465–5506, 2021.
- [76] Lu Lu, Pengzhan Jin, Guofei Pang, Zhongqiang Zhang, and George Em Karniadakis. Learning nonlinear operators via deepnet based on the universal approximation theorem of operators. Nature machine intelligence, 3(3):218–229, 2021.
- [77] Aurélien Lucchi, Karel Smith, Radhakrishna Achanta, Pascal Fua, and Sabine Süsstrunk. Superpixel-based image segmentation using convex optimization. In Proceedings of the IEEE Conference on Computer Vision and Pattern Recognition (CVPR), pages 2089–2096. IEEE, 2011.
- [78] Liam Madden and Christos Thrampoulidis. Memory capacity of two layer neural networks with smooth activations. SIAM Journal on Mathematics of Data Science, 6(3):679–702, 2024.
- [79] Pascal Massart. Concentration Inequalities and Model Selection. Springer, 2007.
- [80] Song Mei and Andrea Montanari. The generalization error of random features regression: Precise asymptotics and the double descent curve. Communications on Pure and Applied Mathematics, 75(4):667–766, 2022.
- [81] Juan Molina, Mircea Petrache, Francisco Sahli Costabal, and Matías Courdurier. Understanding the dynamics of the frequency bias in neural networks, 2024.
- [82] Shay Moran and Amir Yehudayoff. Sample compression schemes for vc classes. Journal of the ACM (JACM), 63(3):1–10, 2016.
- [83] Depen Morwani, Jatin Batra, Prateek Jain, and Praneeth Netrapalli. Simplicity bias in 1-hidden layer neural networks. In A. Oh, T. Naumann, A. Globerson, K. Saenko, M. Hardt, and S. Levine, editors, Advances in Neural Information Processing Systems, volume 36, pages 8048–8075. Curran Associates, Inc., 2023.
- [84] Alireza Mousavi-Hosseini, Adel Javanmard, and Murat A Erdogdu. Robust feature learning for multi-index models in high dimensions. In NeurIPS 2024 Workshop on Mathematics of Modern Machine Learning, 2024.
- [85] Ariel Neufeld and Philipp Schmock. Universal approximation property of random neural networks. arXiv preprint arXiv:2312.08410, 2023.
- [86] Behnam Neyshabur, Srinadh Bhojanapalli, and Nathan Srebro. A PAC-bayesian approach to spectrally-normalized margin bounds for neural networks. In International Conference on Learning Representations, 2018.
- [87] Kushagra Pandey, Ruihan Yang, and Stephan Mandt. Fast samplers for inverse problems in iterative refinement models. Advances in Neural Information Processing Systems, 37:26872–26914, 2024.
- [88] Philipp Petersen and Felix Voigtlaender. Optimal approximation of piecewise smooth functions using deep relu neural networks. Neural Networks, 108:296–330, 2018.
- [89] Philipp Petersen and Jakob Zech. Mathematical theory of deep learning. arXiv preprint, 2024.
- [90] Guergana Petrova and Przemysław Wojtaszczyk. Lipschitz widths. Constructive Approximation, 57(2):759–805, 2023.
- [91] Allan Pinkus. n -widths in approximation theory, volume 7 of Ergebnisse der Mathematik und ihrer Grenzgebiete (3) [Results in Mathematics and Related Areas (3)]. Springer-Verlag, Berlin, 1985.

- [92] Tomaso Poggio, Fabio Anselmi, and Lorenzo Rosasco. I-theory on depth vs width: hierarchical function composition. Technical report, Center for Brains, Minds and Machines (CBMM), 2015.
- [93] Tomaso Poggio and Maia Fraser. Compositional sparsity of learnable functions. Bulletin of the American Mathematical Society, 61(3):438–456, 2024.
- [94] Ali Rahimi and Benjamin Recht. Random features for large-scale kernel machines. In Advances in Neural Information Processing Systems, volume 20, 2007.
- [95] Xiaofeng Ren and Jitendra Malik. Learning a classification model for segmentation. In Proceedings Ninth IEEE International Conference on Computer Vision, volume 1, pages 10–17. IEEE, 2003.
- [96] Erwin Riegler, Alex Bühler, Yang Pan, and Helmut Bölcskei. Generating rectifiable measures through neural networks. arXiv preprint arXiv:2412.05109, 2024.
- [97] Johannes Schmidt-Hieber. Nonparametric regression via deep neural networks. The Annals of Statistics, 48(4):1875–1897, 2020.
- [98] Cornelia Schneider, Mario Ullrich, and Jan Vybíral. Nonlocal techniques for the analysis of deep relu neural network approximations. arXiv preprint arXiv:2504.04847, 2025.
- [99] Cornelia Schneider and Jan Vybíral. A multivariate Riesz basis of ReLU neural networks. Appl. Comput. Harmon. Anal., 68:Paper No. 101605, 16, 2024.
- [100] Matthias Seeger. Pac-bayesian generalisation error bounds for gaussian process classification. In International Conference on Machine Learning (ICML), pages 226–233, 2002.
- [101] Zuowei Shen, Haizhao Yang, and Shijun Zhang. Optimal approximation rate of ReLU networks in terms of width and depth. J. Math. Pures Appl. (9), 157:101–135, 2022.
- [102] Zhongjie Shi, Zhan Yu, and Ding-Xuan Zhou. Learning theory of distribution regression with neural networks. Constructive Approximation, pages 1–44, 2025.
- [103] Taiji Suzuki. Adaptivity of deep reLU network for learning in besov and mixed smooth besov spaces: optimal rate and curse of dimensionality. In International Conference on Learning Representations, 2019.
- [104] Kevin E. Trenberth, John T. Fasullo, and Theodore G. Shepherd. Attribution of climate extreme events. Nature Climate Change, 5:725–730, 2015. Perspective on framing attribution of climate extremes.
- [105] Alexander Tsigler and Peter L Bartlett. Benign overfitting in ridge regression. Journal of Machine Learning Research, 24(123):1–76, 2023.
- [106] Alexander B Tsybakov. Optimal aggregation of classifiers in statistical learning. The Annals of Statistics, 32(1):135–166, 2004.
- [107] A. W. van der Vaart and Jon A. Wellner. Weak convergence and empirical processes—with applications to statistics. Springer Series in Statistics. Springer, Cham, second edition, [2023] ©2023.
- [108] Gal Vardi, Gilad Yehudai, and Ohad Shamir. On the optimal memorization power of reLU neural networks. In International Conference on Learning Representations, 2022.
- [109] Roman Vershynin. High-dimensional probability: An introduction with applications in data science, volume 47. Cambridge university press, 2018.
- [110] Roman Vershynin. Memory capacity of neural networks with threshold and rectified linear unit activations. SIAM Journal on Mathematics of Data Science, 2(4):1004–1033, 2020.
- [111] Paul Viallard, Pascal Germain, Amaury Habrard, and Emilie Morvant. A general framework for the practical disintegration of pac-bayesian bounds. Machine Learning, 113(2):519–604, 2024.
- [112] Eric Volkmann, Alena Brändle, Daniel Durstewitz, and Georgia Koppe. A scalable generative model for dynamical system reconstruction from neuroimaging data. Advances in Neural Information Processing Systems, 37:80328–80362, 2024.

- [113] Dmitry Yarotsky. Error bounds for approximations with deep relu networks. Neural networks, 94:103–114, 2017.
- [114] Dmitry Yarotsky. Optimal approximation of continuous functions by very deep relu networks. In Conference on learning theory, pages 639–649. PMLR, 2018.
- [115] Dmitry Yarotsky. Elementary superexpressive activations. In International conference on machine learning, pages 11932–11940. PMLR, 2021.
- [116] Dmitry Yarotsky and Anton Zhevnerchuk. The phase diagram of approximation rates for deep neural networks. Advances in neural information processing systems, 33:13005–13015, 2020.
- [117] Shijun Zhang, Jianfeng Lu, and Hongkai Zhao. Deep network approximation: Beyond ReLU to diverse activation functions. Journal of Machine Learning Research, 25(35):1–39, 2024.
- [118] Shijun Zhang, Zuowei Shen, and Haizhao Yang. Deep network approximation: Achieving arbitrary accuracy with fixed number of neurons. Journal of Machine Learning Research, 23(276):1–60, 2022.